

Pittsburg State University

Pittsburg State University Digital Commons

Electronic Theses & Dissertations

Graduate School

Spring 5-15-2024

EFFECTS OF NITROGEN, PHOSPHOROUS, AND NITROGEN-PHOSPHOROUS-BASED FLAME RETARDANTS ON PROPERTIES OF BIO-BASED POLYURETHANE FOAM

Janvi Chaudhari

Pittsburg State University, janvibalmukund.chaudhari@gus.pittstate.edu

Follow this and additional works at: <https://digitalcommons.pittstate.edu/etd>

Recommended Citation

Chaudhari, Janvi, "EFFECTS OF NITROGEN, PHOSPHOROUS, AND NITROGEN-PHOSPHOROUS-BASED FLAME RETARDANTS ON PROPERTIES OF BIO-BASED POLYURETHANE FOAM" (2024). *Electronic Theses & Dissertations*. 516.

<https://digitalcommons.pittstate.edu/etd/516>

This Thesis is brought to you for free and open access by the Graduate School at Pittsburg State University Digital Commons. It has been accepted for inclusion in Electronic Theses & Dissertations by an authorized administrator of Pittsburg State University Digital Commons. For more information, please contact digitalcommons@pittstate.edu.

EFFECTS OF NITROGEN, PHOSPHOROUS, AND NITROGEN-PHOSPHOROUS-
BASED FLAME RETARDANTS ON PROPERTIES OF BIO-BASED
POLYURETHANE FOAM

Thesis Submitted to the Graduate School
in Partial Fulfilment of the Requirements
For the Degree of
Master of Science

Janvi Chaudhari

Pittsburg State University

Pittsburg, Kansas

May 2024

EFFECTS OF NITROGEN, PHOSPHOROUS, AND NITROGEN-PHOSPHOROUS-
BASED FLAME RETARDANTS ON PROPERTIES OF BIO-BASED
POLYURETHANE FOAM

Janvi Chaudhari

APPROVED:

Thesis Advisor _____
Dr. Ram K. Gupta, Department of Chemistry

Committee Member _____
Dr. Khamis Siam, Department of Chemistry

Committee Member _____
Dr. Anuradha Ghosh, Department of Biology

Acknowledgments

First and foremost, I would like to thank Dr. Ram K. Gupta for being my instructor and research adviser and for his guidance and support during my study for a master's degree in polymer chemistry. He is the major source of my inspiration, and his hard work and devotion gave me the strength to pursue my goals and aspirations. With his enormous expertise and experience, he guided me in the appropriate direction during my studies. Throughout my master's program, I worked on various projects under his supervision.

I also want to thank Dr. Khamis Siam, and Dr. Anuradha Ghosh for serving on my thesis committee and providing valuable suggestions for molding my thesis appropriately. I am grateful to the National Institute of Materials Advancement, the Department of Chemistry, and Pittsburg State University (PSU) for their financial assistance and scholarships. I would also like to thank Dr. Peter Dvornik, Mr. Paul Herring, and Dr. Jeanne Norton for educating me about polymer chemistry.

Finally, thank you would not be enough for my father, B.L. Chaudhari, who assisted me at every step of my life, and the inspiration he provided cannot be taken away by anything. He reared and cared for me, paying a high price throughout the years to support my education and intellectual development. I don't even have words for my mother, for all of her sacrifices and the countless sleepless hours she spent in my care. Special thanks to my friends Niyati, Sonu, Janu, Mansi, Sagar, Pratik, Niharika, Uday, Jainish, and Nirmal for their academic and moral support, as well as for creating a good and inspirational environment in which I could grow and thrive. I would also like to thank everyone who helped me during my master's degree.

EFFECTS OF NITROGEN, PHOSPHOROUS, AND NITROGEN-PHOSPHOROUS-BASED FLAME RETARDANTS ON PROPERTIES OF BIO-BASED POLYURETHANE FOAM

An Abstract of the Thesis by
Janvi Chaudhari

Rigid polyurethane foams (RPUFs) are widely used materials in buildings, coolers, and refrigerators due to their good thermal insulation properties. They are also used in automobiles due to their low density, sound adsorption, and mechanical properties. However, most of the raw materials used for their production originate from non-renewable sources. Also, these polymers are susceptible to fire due to their porous structure. For that, it is important to incorporate bio-based materials to produce polyurethanes along with flame retardants (FRs) that can efficiently quench a fire and suppress the release of toxic fumes. Herein, soybean oil, henceforth referred to as vegetable oil (VO), was chemically modified to a vegetable oil polyol (VP) through epoxidation and ring-opening reactions which was further characterized by Fourier-transform infrared (FTIR), gel permeation chromatography (GPC), viscosity, and hydroxyl value analysis. Also, nitrogen-phosphorus-based FR synthesized from diphenyl phosphinic acid (DPPA), and melamine (MA) was introduced. For comparison, three different types of FRs were used to make the RPUFs such as MA, dimethyl methyl phosphonate (DMMP), and diphenyl phosphinic melamine salt (DPPMA). Increasing concentrations of the FRs were added to the RPUFs to evaluate their effect on their properties. The physical, thermal, morphological, mechanical, and FR properties of the RPUFs were evaluated. There was a considerable decrease in the horizontal burning time as the control foam (foam without FRs) burnt for 62 seconds whereas after the addition of 23.75 wt.% (12 grams) of MA or DMMP,

separately, the burning time decreased to 7 and 1 seconds, respectively. Upon the addition of 19.54 wt.% (12 grams) of DPPMA, the burning time decreased to 15 seconds.

TABLE OF CONTENTS

CHAPTER I	1
INTRODUCTION.....	1
1.1. Overview of Polyurethane	1
1.2. Basic Chemistry of Polyurethane.....	2
1.3. Classification of Polyurethane	3
1.3.1. Types of Polyurethane.....	3
1.3.2. Raw Material.....	4
1.3.3. Thermal Response.....	5
1.4. Applications of Polyurethanes	5
1.5. Issues of Polyurethane Foams.....	7
1.6. Polyol	8
1.7. Isocyanate	9
1.8. Flame-Retardants	11
1.9. The Objective of this Research	13
CHAPTER II.....	14
MATERIALS AND METHODS.....	14
2.1. Materials	14
2.1.1. Vegetable Oil.....	15
2.1.2. Methylene Diphenyl Diisocyanate.....	15
2.1.3. Catalyst	16
2.1.4. Blowing Agent	16
2.1.5. Surfactant	17
2.1.6. Flame-Retardants	17
2.1.6.1. Melamine	17
2.1.6.2. Dimethyl Methyl Phosphonate	18
2.1.6.3. Diphenyl Phosphinic Melamine Salt	19
2.2. Synthesis of DPPMA Flame-Retardant	19
2.3. Synthesis of Vegetable Oil-Based Polyol	20
2.3.1. Epoxidation of Vegetable Oil.....	20
2.3.2. Ring Opening of Epoxidized Vegetable Oil.....	21
2.4. Characterization of Vegetable Oil-Based Polyol	23
2.4.1. Iodine Value	23
2.4.2. Epoxide Number	23
2.4.3. Hydroxyl Value	24
2.4.4. Acid Value.....	24
2.4.5. Fourier Transform Infrared Spectroscopy.....	25
2.4.6. Viscosity.....	25
2.4.7. Gel Permeation Chromatography	26
2.4.8. ¹ H Nuclear Magnetic Resonance	27
2.5. Preparation of Rigid Polyurethane Foam.....	28
2.6. Characterization of the Foams	30
2.6.1. Apparent Density	30
2.6.2. Closed Cell Content	31
2.6.3. Compressive Strength.....	32

2.6.4. Scanning Electron Microscope	33
2.6.5. Horizontal Burning Test.....	34
2.6.6. Thermogravimetric Analysis.....	35
CHAPTER III	36
RESULTS AND DISCUSSIONS.....	36
3.1. Properties of VO, EVO, and VP	36
3.1.1. Iodine Value	36
3.1.2. Epoxide Number	36
3.1.3. Hydroxyl Value	37
3.1.4. Acid Value.....	37
3.1.5. Viscosity.....	37
3.1.6. Fourier Transform Infrared Spectroscopy.....	38
3.1.7. Gel Permeation Chromatography	40
3.2. Properties of Flame-Retardant	41
3.2.1. Fourier Transform Infrared Spectroscopy of DPPMA FR.....	41
3.2.2. ¹ H Nuclear Magnetic Resonance.....	42
3.3. Properties of the VO-Based RPUFs.....	43
3.3.1. Closed Cell Content	43
3.3.2. Apparent Density	45
3.3.3. Compressive Strength	46
3.3.4. Cell Morphology	48
3.3.5. Thermogravimetric Analysis.....	51
3.3.6. Horizontal Burning Test.....	54
CHAPTER IV.....	59
CONCLUSIONS	59
REFERENCES.....	61

LIST OF TABLES

Table 1:	VO-RPUF formulation with MA and DMMP.....	29
Table 2:	VO-RPUF formulation with MA and DPPMA.....	30
Table 3:	Characterization of vegetable oil, epoxidized vegetable oil, and vegetable oil polyol.....	38

LIST OF FIGURES

Figure 1:	Reaction of isocyanate and polyol.....	3
Figure 2:	Classification of polyurethane.....	3
Figure 3:	Applications of polyurethanes.....	7
Figure 4:	Raw materials for the synthesis of polyether polyol.....	9
Figure 5:	Name and structure of common isocyanate used for the polyurethane.....	11
Figure 6:	The proposed structure of vegetable oil (soybean oil)	15
Figure 7:	Methylene diphenyl diisocyanate.....	16
Figure 8:	Structure of melamine.....	18
Figure 9:	Structure of dimethyl methyl phosphonate.....	19
Figure 10:	Structure of the synthesis of DPPMA.....	20
Figure 11:	Proposed structure of the synthesis of vegetable oil polyol.....	22
Figure 12:	Digital photo of FTIR instrument.....	25
Figure 13:	Digital photo of AR 2000 dynamic stress rheometer	26
Figure 14:	Digital photo of GPC instrument	27
Figure 15:	Digital photo of NMR instrument	28
Figure 16:	Schematic of the preparation of RPUFs.....	29
Figure 17:	Digital photo of Ultracycrometer (Ultrafoam 1000)	31
Figure 18:	Digital photo of Q test 2-tensile machine.....	32
Figure 19:	Digital photo of gold layer sputtering (left), thermo scientific phenom (right).....	33
Figure 20:	Digital photo of horizontal burning test under the fume hood.....	34
Figure 21:	Digital photo of thermogravimetric analysis instrument.....	35
Figure 22:	FTIR spectra of vegetable oil (VO), epoxidized vegetable oil (EVO), and vegetable oil polyol (VP).....	39
Figure 23:	GPC of vegetable oil (VO), epoxidized vegetable oil (EVO), and vegetable oil polyol (VP).....	40
Figure 24:	FT-IR of MA, DPPA and DPPMA.....	42
Figure 25:	NMR of MA, DPPA and DPPMA.....	43
Figure 26:	Closed-cell content of the obtained RPUFs with different weights of (a) MA, (b) DMMP, and (c) DPPMA as FRs.....	44
Figure 27:	The apparent density of the obtained RPUFs with different weights of (a) MA, (b) DMMP, and (c) DPPMA as FRs.....	46
Figure 28:	Compressive strength of RPUFs with different weights of (a) MA, (b) DMMP, and (c) DPPMA FRs.....	48
Figure 29:	SEM images for RPUFs with varying amounts of MA.....	50
Figure 30:	SEM images for RPUFs with varying amounts of DMMP	50
Figure 31:	SEM images for RPUFs with varying amounts of DPPMA.....	51
Figure 32:	Thermal analysis of RPUFs with varying amounts of MA (a) TGA, (b) DTGA.....	53
Figure 33:	Thermal analysis of RPUFs with varying amounts of DMMP (a) TGA, (b) DTGA.....	53

Figure 34:	Thermal analysis of RPUFs with varying amounts of DPPMA (a) TGA, (b) DTGA.....	54
Figure 35:	Comparisons of burning time and weight loss percent of RPUFs with different weights of (a) MA, (b) DMMP, and (c) DPPMA	56
Figure 36:	Digital Photographs of RPUFs before and after the horizontal burning test with different concentrations of MA.....	57
Figure 37:	Digital Photographs of RPUFs before and after the horizontal burning test with different concentrations of DMMP.....	57
Figure 38:	Digital Photographs of RPUFs before and after the horizontal burning test with different concentrations of DPPMA.....	58

LIST OF ABBREVIATIONS

ASTM	American society for testing and materials
DMMP	Dimethyl methyl phosphonate
DPPA	Diphenyl phosphonic acid
DPPMA	Diphenyl phosphinic melamine salt
DTGA	Derivative thermogravimetric analysis
EVO	Epoxidized vegetable oil
FR	Flame retardant
FTIR	Fourier transformed infrared
GPC	Gel permeation chromatography
ISO	International organization for standardization
MA	Melamine
MDI	Methylene diphenyl diisocyanate
PU	Polyurethane
RPUFs	Rigid polyurethane foam
SEM	Scanning electron microscopy
TGA	Thermogravimetric analysis
VO	Vegetable oil
VP	Vegetable oil polyol

CHAPTER I

INTRODUCTION

1.1. Overview of Polyurethane

A polymer is a large molecule made from repeating units of monomers, linked together by covalent bonds. Polymers can be classified based on their structure, source, and properties. They can have a linear, branching, or crosslinked structure. They can also be classified as natural or synthetic polymers [1]. Polyurethane (PU) is one of the most significant groups of polymers. In 1937, E.I. Du Pont and Otto Bayer created the first PU through a polycondensation reaction between alcohol and isocyanate and PU achieved industrial manufacturing scale in the 1940s after some modifications [2]. PUs were initially employed as a substitute for rubber during World War 2 [3]. PUs are versatile polymers that combine the hardness and durability of metals with the softness and durability of rubber, making them an attractive alternative to metals, rubber, and plastic in a wide range of industrial applications. The developments in the field of PUs, as well as their usage in everyday life, have improved the quality of daily life in the modern world. The global polyurethane market was estimated at USD 78.07 billion in 2023 and is predicted to increase at a CAGR of 4.5% from 2024 to 2030 [4]. The global market of PU is growing because of its flexible, chemical, and physical qualities which have been widely employed in several sectors, including construction, footwear, furniture, and textiles, automotive

interiors, packaging, and thermal insulation [5]. PU is an important polymer group because of its many features, including high strength-to-weight ratio, insulation properties, soundproofing, low thermal conductivity, adaptability, and durability. PU characteristics vary depending on the polyol, isocyanate, and additives used in the synthesis.

1.2. Basic Chemistry of Polyurethane

PU is typically formed by the reaction of polyisocyanates and polyol, which results in repeated urethane linkages. **Figure 1** shows the urethane linkage (-NH-COO-) formed by reacting a diisocyanate's isocyanate (-NCO) group with a polyol's hydroxyl group (-OH). To make PU, both starting components must have two or more functionalities. PUs are block copolymers that alternate between soft and hard segments. Soft segments are often made from polyether or polyester polyols, whereas hard segments are created by converting diisocyanate to urethane. PU's versatility originates from its combination of hard and soft segments [6]. The final product's characteristics are influenced by both the polyol and the isocyanate [7–10]. So, modifying the structure of polyols or isocyanates by chemical techniques can result in PUs with diverse characteristics. Using polyols with a linear structure, high molecular weight, and low functionality can produce elastic PUs. Alternatively, a rigid polyurethane can be produced by reacting to a polyol with aromatic groups, low molecular weight, and strong cross-linking capabilities.

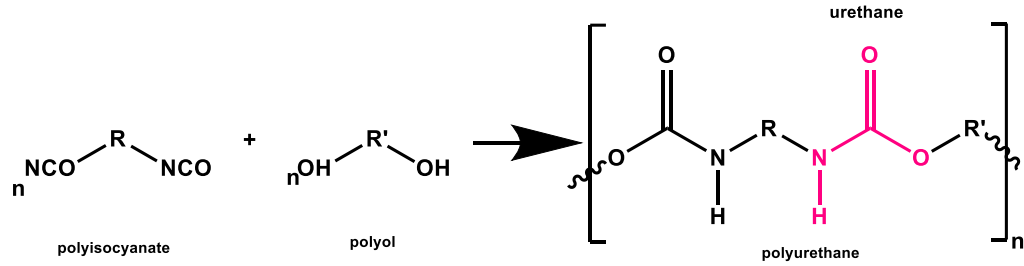


Figure 1. Reaction of isocyanate and polyol.

1.3. Classification of Polyurethane

PUs are so diverse; they are difficult to categorize only by name. The most effective method for identifying and classifying all formats of PUs is illustrated in **Figure 2**.

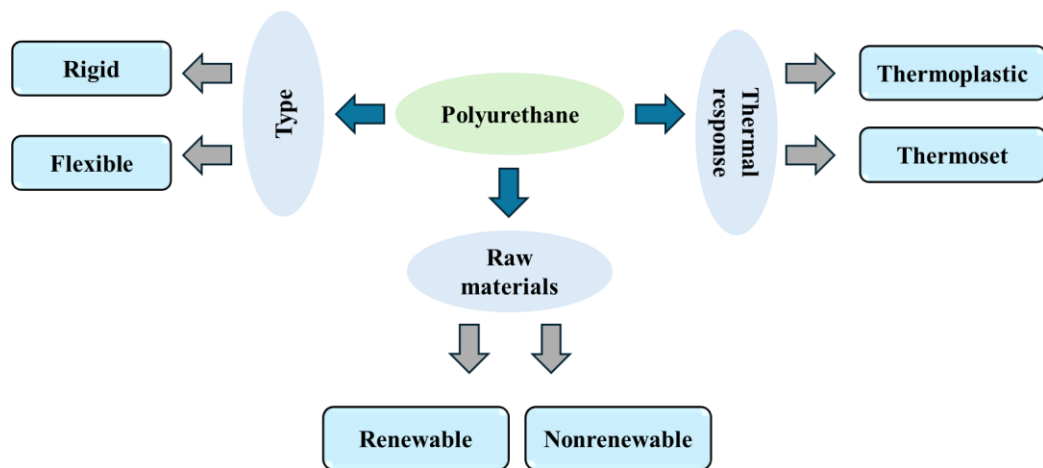


Figure 2. Classification of polyurethane.

1.3.1. Types of Polyurethane

PUs can be characterized as rigid, flexible, thermoplastic, adhesives, coating, binders, elastomers, and sealants due to the variety of sources from which they can be synthesized and their distinguished usage. In which flexible polyurethane foams (FPUFs) are the most widely produced PU, accounting for 31% of total output, because of their

flexibility, durability, and light weight, good surface elasticity, they are commonly employed in applications that need cushioning and comfort like mattresses and bedding, seatings of automotive, soundproofing applications, furniture [11]. Flexible polyurethanes have an open-cell structure, allowing air to circulate freely [12]. RPUFs are the second most popular form of PU, accounting for 25% of manufacturing, due to their insulating characteristics, structural stability, light weight, and low density [11]. Because of its outstanding thermal insulating capabilities and structural stability, it is widely utilized in a variety of applications, including construction, roofing, and wall insulation, and kitchen appliances like refrigerators and freezers [13]. Aside from building, these foams are utilized in furniture, vehicle insulation, refrigeration transportation, cold storage, pipeline insulation, and soundproofing. RPUFs have more than 90% closed cell content, which prevents air from flowing out of the foams and so provides good thermal insulation.

1.3.2. Raw Material

PU is generally manufactured with diisocyanate and polyol. Typically, both of those chemicals are generated from petroleum feedstocks, leading to issues such as price fluctuation, insufficient feedstock, dangerous chemical pollution, and raised emissions of greenhouse gases [14]. As a result, numerous studies have been conducted to produce an environmentally friendly alternative to petroleum-based materials. Nowadays, bio-based materials are in demand due to several benefits such as eco-friendliness, biodegradability, low cost, and non-toxicity. Compared to petroleum-based products, agricultural products like vegetable oils are both sustainable and ecologically beneficial. Bio-polyols have been synthesized successfully from renewable feedstocks, including fatty acids, vegetable oils,

and protein-based resources [15–23]. There are only a few reports on synthesizing bio-based isocyanates.

1.3.3. Thermal Response

Polymer's response to heat and chemical reactions differs into two main categories: thermoplastics, and thermosets. Thermoplastic polymers are a combination of linear or branched chains held together by weak forces such as van der Waals forces. They can be melted or softened when heated and solidified and retain their new structure after cooling. Heating thermoplastic polymers results in reversible behavior without considerable property deterioration. Thermoplastic polymers provide several advantages, including low chemical change before and after processing, ductility, and recycling possibilities [24]. In contrast, thermoset polymers consist of a crosslinked or network structure made up of strong covalent bonds and once they crosslinked, they cannot be reshaped. Thermoset polymers have no melting point and deteriorate in response to heat. Thermoset polymer undergoes permanent chemical change during the curing process, and because of the crosslinked network, it has higher strength, stiffness, and heat resistance than thermoplastic polymers.

1.4. Applications of Polyurethanes

PU's can be employed in many goods, such as paints, coatings, waterborne PU's [25], elastomers [26], elastic fibers, flexible and rigid foam [27], adhesives [28–30], and sealants utilizing different starting compounds and different syntheses [31]. Foams contribute to about 68% of all PU applications [32], which are divided into two categories: flexible foam and rigid foam. Their uses differ due to differences in structure, density, and

flexibility. Flexible foams are commonly utilized in applications such as mattresses, sofas, automobile seats, and automotive interior design, footwear, carpet underlay where comfort and cushioning are vital due to their flexibility [33]. On the other hand, because of their particular benefits like low cost, long life, and reduced carbon emissions, rigid foams are the second most common PU which are used in applications requiring insulation such as insulation panels, freezers and refrigerators, building insulation, furniture, and energy-efficient transportation [34]. Elastomers are rubber-like compounds with strong elasticity and durability. They are utilized in a variety of applications, including automotive (tires), medical equipment (e.g., cardiac-assist pumps and blood bags), and chronic implants (e.g., heart valves and vascular grafts), due to their capacity to deform and return to their original shape after stress [26]. PU adhesives are durable, solvent-resistant, cohesive, and abrasion-resistant. So its uses include wood flooring, construction and building materials, the automotive industry, electronics and electrical applications, packaging and labeling, and medical and healthcare [35]. PU coatings provide abrasion, chemical, weather, and UV resistance and are used in a variety of applications, including architectural coatings (exterior and interior paints), automotive coatings, industrial coatings (marine, oil and gas, and chemical processing industries), and wood coatings. **Figure 3** illustrates the common applications of polyurethanes.

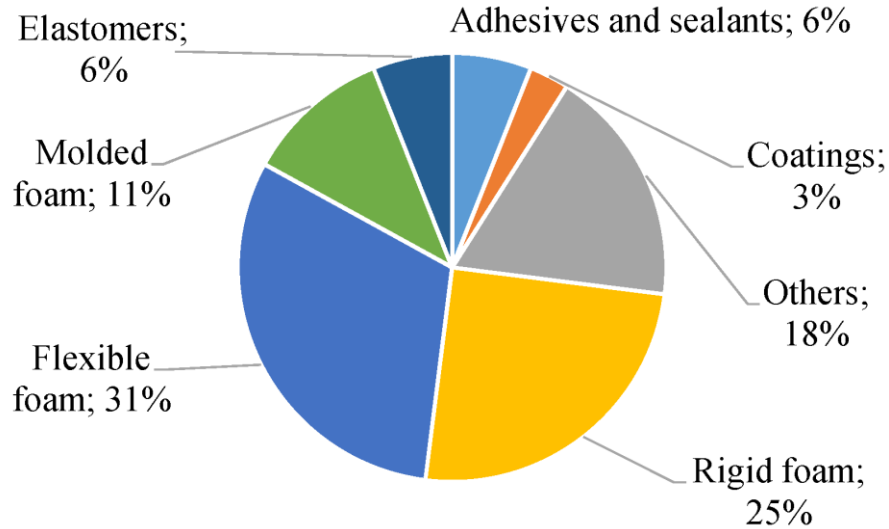


Figure 3. Applications of polyurethanes. Reproduced with permission [11].

Copyright 2018 by the authors. Licensee MDPI, Basel, Switzerland. This article is an open access article distributed under the terms and conditions of the Creative Commons Attribution (CC BY) license.

1.5. Issues of Polyurethane Foams

A large concentration of soft segments in the polyethylene chain, a porous structure, low density, and low thermal inertia, PU foams are extremely flammable when exposed to heat [36]. Because of oxygen deprivation in fire victims, poisonous gases such as CO, CO₂, and HCN are produced from the burning of PU foam, which are hazardous to human health and the environment. FRs are an effective way to lower the flammability of foam. FRs can prevent the spread of fires by physical and/or chemical interference [37]. Another major challenge confronting the PU industry is the usage of polyols and isocyanate produced from petrochemical sources. As a result, initiatives are being conducted to develop inexpensive, biobased, and renewable sources for polyol synthesis [38]. Another issue with PU production is isocyanate, which is produced from the hazardous chemical phosgene.

Long-term isocyanate exposure has adverse effects on the respiratory system and causes skin irritation and sensitization [39].

1.6. Polyol

Polyols are the primary starting material for PU manufacturing and are molecules containing more than two hydroxyl groups. The hydroxyl groups allow the polyol to react with isocyanate [40]. Polyester and polyether are the two major types of polyols, accounting for more than 80% of polyol production. Polyether polyols are produced from ethylene, propylene, or butylene oxides as the primary starting components. The structures are illustrated in **Figure 4**. Polyether polyol combines ether linkages and a hydroxyl group in one backbone, and because of its flexibility, low viscosity, and excellent hydrolytic stability, it is compatible with a variety of additives and fillers used in PU production. Polyester polyols, on the other hand, are formed by the esterification of diols or polyols with dicarboxylic acids or their derivatives. Polyester polyol synthesis utilizes ethylene glycol, propylene glycol, and butanediol as starting elements and has ester linkages and a hydroxyl group in its structure. Other polyols that can be used in PU synthesis include polycarbonate polyols and acrylic polyols. The nature, functionality, and molecular weight of polyols impact PU properties and applications. To produce flexible or elastic PUs, linear chains with low functionality (2-4) and low degree of cross-linking, as well as high molecular weight polyols with long alkyl segments, are employed. In this regard, polyols with low molecular weight, a high degree of crosslinking, short chains, and high functionality (3-8) are another important class of precursor chemicals to produce rigid polyurethanes. They increase the viscosity, resulting in highly branched and cross-linked PUs.

Most of the polyols used in the manufacturing of PUs originate from petroleum resources. There are discussions on using alternate sources to ensure a more consistent and inexpensive supply while simultaneously solving environmental issues and economic instability. There are several issues associated with petroleum-based materials, including the depletion of global crude oil, environmental concerns, and the volatility of crude oil expenses. However, there has been significant development in employing bio-renewable resources to synthesize polyols [20,22]. Vegetable oils derived from soybean, canola, castor plant, and rapeseed, as well as walnut shells and lignin [41] are being investigated as starting materials for polyol synthesis. They are inexpensive, readily available, ecologically benign, and sustainable alternatives to petroleum-based polyol. This vegetable oil can be chemically functionalized due to the presence of unsaturated carbon-carbon double bonds, which allow the introduction of hydroxyl groups [42–44]. Such a process can be performed through several techniques such as epoxidation/ring-opening, hydroformylation, amidation, thiol-ene coupling, and ozonolysis to name some [45–47].

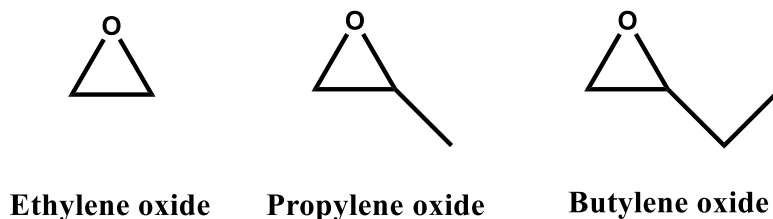


Figure 4. Raw materials for the synthesis of polyether polyol.

1.7. Isocyanate

The other major component used in PU production is isocyanates. Organic compounds containing an isocyanate group ($R-N=C=O$) are called isocyanates.

Isocyanates used in PU synthesis are often bifunctional (diisocyanates). These compounds are very reactive and can undergo several reactions with groups containing active hydrogen [31]. PUs are commonly produced using two types of isocyanates: aliphatic and aromatic isocyanate. **Figure 5** shows the structure of various isocyanates. Aliphatic isocyanates include isophorone diisocyanate (IPDI) and hexamethylene diisocyanate (HDI), both of which include aliphatic carbon chains right after the isocyanate functional group. However, aromatic isocyanates, such as toluene diisocyanate (TDI) and diphenylmethane diisocyanate (MDI), have aromatic carbon chains next to the isocyanate functional group. Aliphatic isocyanates are often less reactive than aromatic isocyanates and produce a more uniform response kinetics, so PU manufacture typically uses less aliphatic isocyanates than aromatic isocyanates. The molecular structure of isocyanates can vary from rigid to flexible, which can affect the final characteristics of PUs. Aliphatic isocyanates are commonly used in applications requiring outdoor exposure or color permanence, such as automotive coatings, architectural coatings, and flooring because they impart unique properties such as high flexibility, weather resistance, and light stability to the final product. Aromatic isocyanates are frequently used in applications including RPUFs and FPUFs, coatings, adhesives, sealants, and elastomers because of their high strength, chemical resistance, and thermal stability to the end products.

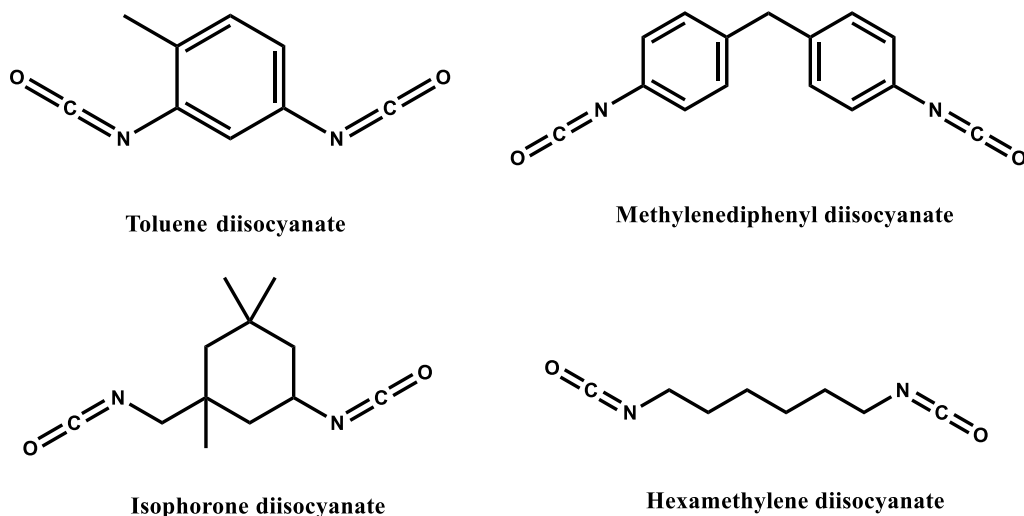


Figure 5. Name and structure of common isocyanates.

1.8. Flame-Retardants

The high porosity of PU foams, which results from air permeation within the structure makes them susceptible to fire. Consequently, there is a need to increase the flame retardancy of PU foams without losing their intrinsic features. For this purpose, FRs are introduced into PU foams. Two types of FRs are frequently used in PU foams: additives and reactive FRs [18,21,48,49]. Additive FRs can be physically blended into the PU during the mixing step, which is typically a less expensive and more effective method of introducing a larger number of FRs. These are not part of the chemical structure of PU but instead are added to polymer materials to improve ignition resistance and minimize flame spread, heat release, and smoke and fume formation. However, in some cases, the addition of significant quantities of FR leads to deterioration properties due to incompatibility with the PU matrix, which is compounded by microphase separation [37]. The reactive FRs provide flame retardancy primarily by chemical interaction with the polymer

backbone. Even distribution of FR throughout the foam matrix allows for constant flame retardancy, throughout the materials, and maintains the flame retardancy over time because the FRs neither migrate nor leach [21,50]. The primary disadvantages of reactive FRs are (1) Adding a synthetic step increases costs and (2) may result in a dangling group on the chain, reducing mechanical strength owing to the plasticizer effect [51].

Furthermore, FRs are classified into two categories: halogenated FRs and halogen-free FRs. Halogen FRs (e.g., chlorine, bromine, fluorine, and iodine) are effective and low-cost. However, their higher toxicity and the formation of potentially carcinogenic halogenated furans and dioxins during combustion can be harmful to the environment and human health. Recent research has focused on generating halogen-free FRs to replace halogenated ones. Phosphorus and nitrogen-based intumescent technologies are especially desired. Examples of halogen-free FRs include phosphorous, nitrogen, and phosphorous-nitrogen-based salts such as ammonium polyphosphate, red phosphorus, melamine phosphate, melamine, and its derivatives such as melamine cyanurate, and ammonium polyphosphate-melamine [52]. Halogen-free FRs have various advantages, including being environmentally benign, less hazardous, improving fire resistance, and being compatible with other materials. FR acts as a "heat sink" by absorbing heat from its surroundings and undergoing an endothermic process. The FR creates a stable char layer that separates the combustible material and releases inert gases including CO₂, NH₃, and H₂O. These gases diminish the concentration of oxygen and cool the system. Chemical reactions occur in two physical states: gaseous and condensed. The gas-phase process occurs when a FR releases volatile radical fragments, such as Cl●, Br●, PO●, and PH₂●. Scavenging H● and OH● plays a crucial role in producing stable volatile or less reactive

compounds, depriving the combustion reaction of oxygen. The condensed phase method involves the FR forming a compact char layer that functions as a shield, preventing oxygen and radical species from entering the PU. The char layer consists of both the thermal degradation of the FR and the degraded polymer [27].

1.9. The Objective of this Research

Here, a vegetable oil-based polyol was developed utilizing a simple epoxidation process, followed by a ring-opening reaction. This study aims to enhance the fire resistance of RPUFs by using nitrogen, phosphorous, and nitrogen-phosphorous-based FRs as non-halogenated FRs using bio-based polyols. Confirmatory tests such as Fourier-transform infrared (FTIR), hydroxyl value, gel permeation chromatography (GPC), and others were performed to investigate the formation of the bio-based polyol before the foam production process. Three types of FRs, melamine (MA), dimethyl methyl phosphonate (DMMP), and diphenyl phosphinic melamine salt (DPPMA) were applied individually in varying concentrations to investigate their effects on the foam's characteristics like flammability, closed cell content, thermal and mechanical properties. Other foam properties such as density and microstructure were also investigated.

CHAPTER II

MATERIALS AND METHODS

2.1. Materials

Vegetable oil (VO) was obtained from a local Walmart in Pittsburg, Kansas, USA to synthesize VP. Along with this, other chemicals like, glacial acetic acid (99.7%), hydrogen peroxide (29%), toluene (99.5%), Amberlite IR 120H, sodium chloride (99.9%), sodium sulfate (99.9%), tetrafluoro boric acid (48 wt.%), Lewitt MP64 (99.8%), and methanol (99.9%) were purchased from Fisher Scientific (Allentown, PA, USA). Jeffol SG-522 (sucrose polyol with OH# 522) and Rubinate M isocyanate (methylene diphenyl diisocyanate) were gifted by Huntsman (The Woodlands, TX, USA). Distilled water used as a blowing agent was purchased from the local Walmart (Pittsburg, KS, USA), and silicone surfactant B8404 was obtained from Evonik (Parsippany, NJ, USA). Air Products in Allentown, PA, USA supplied the catalysts 1,4-diazabicyclo [2.2.2]octane (DABCO) and dibutyltin dilaurate (DBTDL). The FRs melamine (99%) and dimethyl methyl phosphonate (97%) were purchased from Sigma Aldrich (St. Louis, MO, USA). For the synthesis of DPPMA FR, the diphenyl phosphonic acid (DPPA) was obtained from Fisher Scientific (Allentown, PA, USA). Ethyl alcohol (99.5%) used as a solvent was purchased from Sigma Aldrich (St. Louis, MO, USA).

2.1.1. Vegetable Oil

VO can be produced from a wide range of plant sources, including seeds, nuts, fruits, and grains. VO's fundamental structure consists of three fatty acid chains esterified to a glycerol molecule. These include saturated fatty acids, monounsaturated fatty acids, and polyunsaturated fatty acids. Chemical processes such as epoxidation, ozonolysis, hydrogenation, hydroformylation, and thiol-ene coupling may easily change the unsaturation site of any oil [20,22,48,53]. In this study, VO's carbon-carbon double bonds were transformed into an epoxide group via the epoxidation procedure, and methanol was added during the ring-opening step to produce the bio-based polyol. Polyol can react with the isocyanate to generate the urethane linkage during the PU formation of the foaming process. Aside from this bio-based polyol, Jeffol SG-522 was also employed during foam production, which is a commercially available polyol with a hydroxyl number of 522 mg KOH/mg. The proposed structure of VO is shown in **Figure 6**.

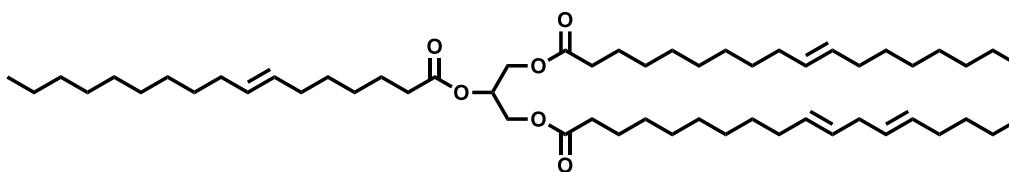


Figure 6. The proposed structure of vegetable oil (soybean oil).

2.1.2. Methylene Diphenyl Diisocyanate

Isocyanates are a crucial component in the synthesis of polyurethane, and because of their strong reactivity with active hydrogens, they must be handled with particular caution [54]. Furthermore, several aliphatic and aromatic isocyanates are available in the

market, however, because aromatic isocyanate has a greater reactivity, compared with aliphatic isocyanate, TDI and MDI are widely used. MDI was employed to generate RPUFs in this study because it has good homogenous reaction kinetics and is less detrimental to work with due to its lower vapor pressure than other isocyanates [55]. In **Figure 7**, the chemical structure of MDI is displayed. It has a weight equivalence of 135, functionality of 2.7, and viscosity of 0.21 Pa.s and contains 31% reactive NCO groups.

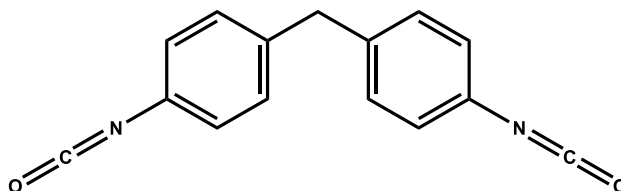


Figure 7. Chemical structure of methylene diphenyl diisocyanate.

2.1.3. Catalyst

Catalysts are substances that accelerate the rate of a reaction without being consumed by themselves. Tertiary amines, organometallic catalysts, quaternary ammonium salts, and alkali metal carboxylates are the four primary types of catalysts that could be utilized in the creation of PU foams. In this study, dibutyltin dilaurate, an organo-tin catalyst, and 1,4-diazobicyclo[2.2.2]-octane, a tertiary amine, were utilized.

2.1.4. Blowing Agent

Blowing agents are used in the production of PU foams to form a regular cellular structure and reduce density during the foaming process. Distilled water was used as a blowing agent in this experiment owing to its low price, non-harmful nature, and ease of accessibility. When water reacts with isocyanate functionalities, an unstable carbamic acid

emerges, which immediately decomposes to generate an amine and carbon dioxide (CO₂) which aids in the expansion of PU foams [56].

2.1.5. Surfactant

Surfactants, which reduce the surface tension of the developing gas-liquid interface, stabilize the foam immediately following the mixing of the polyol and isocyanate. They inhibit the formation of air bubbles in foam, which can lead to the collapse of cells and foam. Surfactant plays an important function in obtaining open and closed cell structures during PU foam production since they greatly impact foam properties. In general, silicone surfactants are commonly used in the polyurethane industry. In this study, B8404 was used as a surfactant during the production of PU foams.

2.1.6. Flame-Retardants

FRs are compounds that are resistant to fire during combustion. In general, there are two types of FRs on the market: additive FRs and reactive FRs. Reactive FRs provide flame retardancy via chemical bonding with the backbone of polymer. However, the additional FRs can be physically integrated into the PU during the mixing step [37]. Herein, in this study, three different types of additive FRs are utilized because they are a more affordable, more easily accessible, and more effective means to introduce more than one type of flame retardant.

2.1.6.1. Melamine

Melamine (2, 4, 6-tri amino-1, 3, 5 triazine) and its derivatives are the most common organic nitrogen compounds used as additives FRs in PU foams. Nitrogen compounds are small but quickly developing subclass of FRs that are attracting public

attention as environmentally benign FRs. Their primary benefits are low toxicity, solid state, and in the case of a fire, the lack of hazardous gases and minimal smoke development [57]. MA is a solid white crystalline substance with a nitrogen content of 67%. MA decomposes at high temperatures due to the removal of ammonia, which dilutes oxygen and combustible gases and leads to the development of thermally stable condensates known as melam, melem, and melon [51]. Melam, melem, and melon production create residues in the condensed phase resulting in endothermal processes, which are also useful for flame retardancy. The structure of MA is illustrated in **Figure 8**.

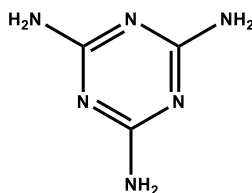


Figure 8. Structure of melamine.

2.1.6.2. Dimethyl Methyl Phosphonate

DMMP is a colorless liquid that is soluble in water (**Figure 9**). DMMP is a very effective halogen-free flame retardant that may greatly enhance the limiting oxygen index (LOI) [58]. It is one of the most efficient phosphorus containing FRs. Furthermore, its properties, which include lower molecular weight, low viscosity, good solubility, a high phosphorus content, and non-corrosive abilities, make it more appropriate for use in polymer materials [59].

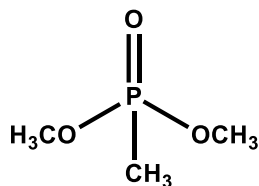


Figure 9. Structure of dimethyl methyl phosphonate.

2.1.6.3. Diphenyl Phosphinic Melamine Salt

DPPMA FR functions by a variety of processes, including the production of flame-inhibiting gases, char formation, and interference with the combustion process. DPPMA was created by a simple reaction between MA and DPPA. With increasing temperature, DPPA generates gaseous products containing phosphorus and benzene, which could produce polyphosphoric acid and phosphorus-containing radicals, and MA produces polymeric products such as melam, melem, and melon, as well as NH_3 to dilute the combustible gas which enables the char layer on foam and protect the foam from burning [60].

2.2. Synthesis of DPPMA Flame-Retardant

In a three-neck round bottom flask, 44 grams of DPPA was mixed in a combination of the solvents water (500 ml) and ethanol (250 ml) for 4 hours with the help of a mechanical stirrer at $90\text{ }^\circ\text{C}$ in an oil bath. A condenser was attached to the three-neck flask. Next, 20.16 grams of MA was added to the solution, and the reaction was allowed to continue for 24 hours. Afterward, the temperature was reduced to $50\text{ }^\circ\text{C}$ at this time the white precipitate was generated in the mixture. Thereafter, the solution was filtered, and

the white precipitate of DPPMA was completely dried in the oven at 50 °C for another 24 hours. The synthesis of DPPMA is depicted in **Figure 10**.

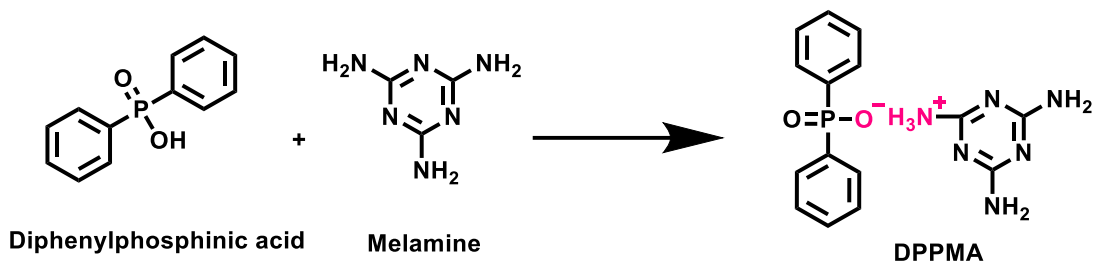


Figure 10. Synthesis of DPPMA using diphenylphosphinic acid and melamine.

2.3. Synthesis of Vegetable Oil-Based Polyol

2.3.1. Epoxidation of Vegetable Oil

In general, four processes are followed to generate epoxides from olefinic-type molecules: (i) epoxidation with percarboxylic acids, (ii) epoxidation with organic and inorganic peroxides, (iii) epoxidation with halohydrins, and (iv) epoxidation with molecular oxygen. Herein, we performed the most common method for this work: the reaction of an alkene with peracetic acid (the epoxidation with percarboxylic acid). Epoxidation processes are frequently carried out with in-situ peracid production due to their high conversion and feasibility on an industrial scale. Peracetic acid is formed when acetic acid and hydrogen peroxide interact, which further breaks the oil's double bonds into an epoxide ring [61,62].

In a three-neck round bottom flask (21), 500 grams of VO, 125 grams of Amberlite IR 120H resin (25 wt.% of VO), and 250 ml of toluene (50 wt.% of VO) were thoroughly stirred with the help of a mechanical stirrer at room temperature for 15 to 20 minutes to

make the system homogeneous. After that, the mixture was cooled down to 5 to 10 °C with ice cubes. Then, using a dropping funnel, 75 ml of glacial acetic acid was added in a dropwise manner into the mixture and stirred for another 30 minutes. After adding the 30% H₂O₂ (423 ml), the mixture was stirred for another 7 hours at 70 °C. After 7 hours, the mixture was allowed to cool to ambient temperature before being filtered to extract the resin from the oil. The mixture was then washed with 10% brine solution 7 to 8 times in the separating funnel. During the washing, the mixture was left to sit for 20 to 30 minutes to allow the oil and water layers to separate. Later, approximately 3 grams of anhydrous sodium sulfate was added to the oil to remove entrapped moisture from the oil and stirred for another 15 minutes. Finally, the rotary evaporation of the oil was done at low and high vacuums, respectively to remove the solvents from the oil.

2.3.2. Ring Opening of Epoxidized Vegetable Oil

In this study, methanol was used to accelerate the ring-opening of the epoxide, resulting in the formation of hydroxyl functional groups. The nucleophile in this reaction was methanol, while the catalyst was tetrafluoroboric acid. The mole ratio of methanol and epoxidized vegetable oil (EVO) was 7:1. The weight of tetrafluoro boric acid was 0.05 wt.% of the total weight of methanol and epoxidized oil. At a temperature of approximately 70 °C, the reaction mixture of methanol and tetrafluoroboric acid was prepared in a three-necked flask connected to a condenser and dropping funnel. The previously synthesized EVO was added dropwise into the flask with the dropping funnel and the mixture was stirred for another hour. Later, the mixture was allowed to cool down to room temperature before adding the Lewitt MP 64 ion exchange resin into the oil which was stirred for another 35-40 minutes to neutralize the acid. The solution was filtered to remove the resin

after verifying that the pH was neutral followed by rotary evaporation to remove the remaining solvents. **Figure 11** depicts the overall structural and bond changes that occur throughout the polyol synthesis from VO, which involves both epoxidation and ring-opening processes.

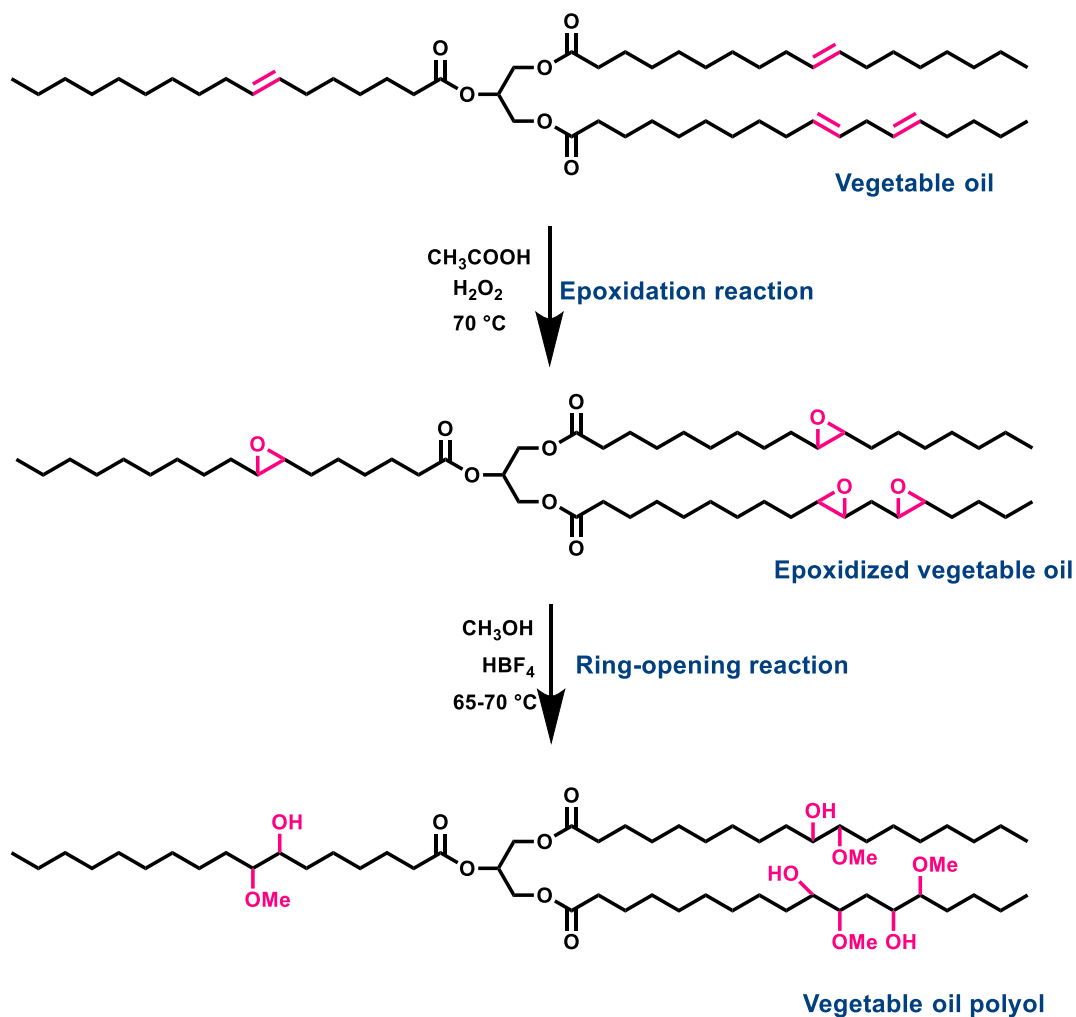


Figure 11. Synthesis of vegetable oil polyol.

2.4. Characterization of Vegetable Oil-Based Polyol

2.4.1. Iodine Value

The number of double bonds in the unsaturated molecule was evaluated by the iodine value that interacts with 100 grams of VO. A high iodine value indicates that the fatty acids have a significant level of unsaturation [63]. The Hanus method was employed in this experiment to determine the amount of double bonds in the VO used to synthesize the polyol. In a 250-ml Erlenmeyer flask, approximately 0.21 grams of VO was dissolved with 10 ml of chloroform (CHCl_3). After a gentle shake, 20 ml of Hanus reagent (BrI) was added to the solution, which was then placed in the dark for an hour. Following that, 20 ml of a 10% potassium iodide (KI) solution and 50 ml of HPLC-grade water were added to the flask and stirred to create a homogeneous solution. Six drops of starch indicator were then added, and the red solution was titrated with sodium thiosulphate ($\text{Na}_2\text{S}_2\text{O}_3$) until a clear (colorless) solution was obtained.

2.4.2. Epoxide Number

Using tetraethylammonium bromide (TEAB) and glacial acetic acid the epoxy oxygen content (EOC%) was calculated. In this experiment, 0.2 grams of EVO was dissolved into a 50 ml solution of tetraethylammonium bromide and agitated for 10 minutes. A drop of crystal violet indicator was then added, and the mixture was titrated with 0.1 N perchloric acid (HClO_4). When the color transformed from blue to green, the titration was complete. The recorded volume was then used to calculate the epoxy content of the EVO.

2.4.3. Hydroxyl Value

The hydroxyl number (OH) of a polyol is a significant indicator of its functionality and used to calculate the precise quantity of isocyanate required for a successful chemical reaction. In this experiment, the OH number of vegetable oil polyol (VP) was evaluated using the phthalic anhydride pyridine (PAP) procedure according to ASTM-D 4274. Here, 10 ml of a hydroxyl solution was added to 0.6 grams of the synthesized vegetable oil polyol within a glass bottle. The bottles, loosely closed, were put in a preheated oven at 100 °C for 70 minutes, with some shaking every 15 minutes. The mixture was subsequently brought to room temperature before 10 ml of HPLC-grade water and 20 ml of isopropanol were added. Following 10 minutes of stirring, 1 N potassium hydroxide (KOH) was gradually added and titrated until a pink color appeared. The volume was recorded and used to calculate the hydroxyl number.

2.4.4. Acid Value

The acid value has been assessed at various stages during the polyol synthesis to achieve the correct pH values necessary for polyurethane foam formation. This identification was carried out using the IUPAC 2.201 standard procedure. A 30 ml solvent combination of isopropanol, toluene, and a phenolphthalein indicator was used to dissolve about 3 grams of the sample. The solution was then titrated with 0.1 N potassium hydroxide until a pink color change was identified. The acid amount was calculated using the volume measured during the titration.

2.4.5. Fourier Transform Infrared Spectroscopy

FTIR is a quick and easy way to detect different functional groups in a chemical compound. FTIR spectra of the samples were recorded using a PerkinElmer Spectrum Two Spectrophotometer (**Figure 12**). The samples were scanned with an average of 64 scans in the wavelength range of $4000\text{-}400\text{ cm}^{-1}$ at a resolution of 4 cm^{-1} , allowing for a quick and complete investigation of the chemical components.



Figure 12. Digital photo of FTIR instrument.

2.4.6. Viscosity

A material's viscosity is a significant indicator of its flow resistance, revealing a variation in molecular weight. Low viscosity denotes a low molecular weight, whereas high viscosity denotes a high molecular weight. Furthermore, increased processibility is associated with lower viscosity. In application, the viscosity of the vegetable oil polyol will

impact the ease of polyurethane synthesis in this experiment. This measurement will also confirm the accurate polyol synthesis utilizing VO epoxide. The analysis was performed using an AR 2000 dynamic stress rheometer (TA Instruments, USA), as illustrated in **Figure 13**. The viscosity was measured at 25 °C with shear stress increasing from 1 to 2000 Pa linearly. The dynamic rheometer was equipped with a cone plate having an angle of 2° and a cone diameter of 25 mm.



Figure 13. Digital photo of AR 2000 dynamic stress rheometer.

2.4.7. Gel Permeation Chromatography

In this size-exclusion method, molecules are distributed based on their excluded volume, which corresponds to their molecular weight. This characterization approach was used to test and validate the vegetable epoxide and polyol generated from the oil following the epoxidation and ring-opening reactions. The Waters GPC instrument from Milford,

MA, USA, was used for this project (**Figure 14**). The instrument employs a variety of pore diameters to help separate molecules with differing molecular weights. The GPC instrument was assembled up of four Phenogel columns measuring 300×7.8 mm and having different pore sizes: 50, 102, 103, and 104 Å. The eluent solvent was tetrahydrofuran, with a constant eluent rate of 1 ml/min at 30 °C. This arrangement ensured that the components of interest were effectively separated and analyzed.



Figure 14. Digital photo of GPC instrument.

2.4.8. ^1H Nuclear Magnetic Resonance

Nuclear Magnetic Resonance (NMR) equipment is used to investigate the molecular structure, dynamics, and interactions of diverse chemical substances. The Magritek spinsolve 80 Multi X NMR spectrometer was utilized to perform ^1H NMR in this study as illustrated in **Figure 15**. Dimethyl sulfoxide was utilized as the solvent. The investigations used 80 MHz proton NMR at room temperature.



Figure 15. Digital photo of NMR instrument.

2.5. Preparation of Rigid Polyurethane Foam

A one-shot free-forming procedure was used to create bio-based RPUFs, which included polyol and isocyanate, as well as a catalyst, surfactant, blowing agent, and flame-retardant. The calculated amount of SG-522, synthesized VP, and different amounts of FRs were poured into a plastic cup and mixed with the mechanical stirrer to make it homogeneous for 1 minute. Along with these, the catalysts, blowing agent, and silicone surfactant were added and mixed with a mechanical stirrer until it became a uniform mixture. Later, the isocyanate was poured into the mixture and thoroughly stirred for another 30 seconds. The resulting polyurethane foams were cured at room temperature for seven days before performing any testing. The schematic of the preparation of RPUFs is illustrated in **Figure 16**.

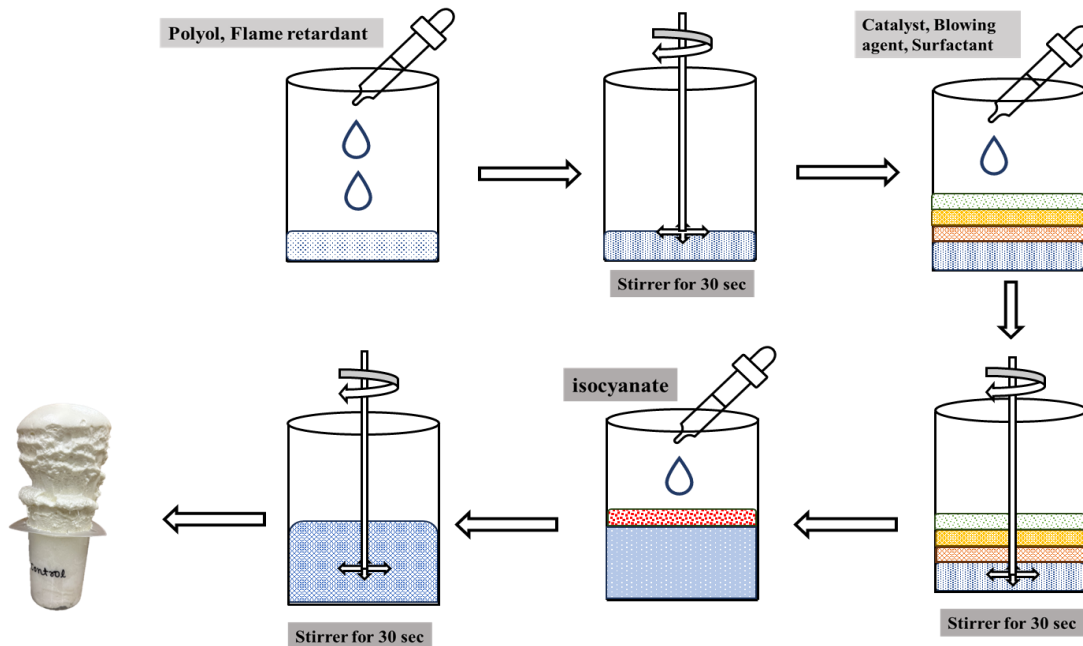


Figure 16. Schematic of the preparation of RPUFs.

Table 1. VO-RPUF formulation with MA and DMMP. All numbers are in grams except wt.% of MA and DMMP.

Ingredients	MA-0	MA-1	MA-2	MA-5	MA-7	MA-10	MA-12
VO-Polyol	10	10	10	10	10	10	10
SG-522	10	10	10	10	10	10	10
A-1	0.18	0.18	0.18	0.18	0.18	0.18	0.18
Water	0.8	0.8	0.8	0.8	0.8	0.8	0.8
T-12	0.04	0.04	0.04	0.04	0.04	0.04	0.04
B8404	0.4	0.4	0.4	0.4	0.4	0.4	0.4
Isocyanate	29.1	29.1	29.1	29.1	29.1	29.1	29.1
MA, DMMP	0	1	2	5	7	10	12
Wt % of MA, DMMP	0	1.97	3.95	9.89	13.85	19.79	23.75

Table 2. VO-RPUF formulation with DPPMA. All numbers are in grams except wt.% of DPPMA.

Ingredients	DPPM A-0	DPPM A-1	DPPM A-2	DPPM A-5	DPPM A-7	DPPM A-10	DPPM A-12
VO-Polyol	10	10	10	10	10	10	10
SG-522	10	10	10	10	10	10	10
A-1	0.18	0.18	0.18	0.30	0.40	1.45	1.45
Water	0.8	0.8	0.8	0.8	1.2	1.4	1.4
T-12	0.04	0.04	0.04	0.08	0.12	0.16	0.16
B8404	0.4	0.4	0.4	0.4	0.4	0.4	0.4
Isocyanate	29.1	29.1	29.1	29.1	29.1	29.1	29.1
DPPMA	0	1	2	5	7	10	12
Wt % of DPPMA	0	1.97	3.95	9.86	12.23	16.28	19.54

2.6. Characterization of the Foams

The apparent density, closed cell content, microstructure, compressive strength, flammability, and thermal behavior were studied to characterize the physiochemical, mechanical, and thermal properties of the produced RPUFs. In the apparent density, closed cell content, and compressive strength testing, a cylindrical sample of each RPUF with approximate dimensions of 45 mm diameter and 30 mm height was used.

2.6.1. Apparent Density

The apparent density is important because it provides information about the physicochemical properties of the foam. Apparent density can be calculated by dividing mass by volume. The internal volume of pores dispersed within a cross-linked matrix affects foam density. In this investigation, the density of RPUF was calculated using the ASTM D1622 standard.

2.6.2. Closed Cell Content

Foams are classified according to their cell structure, which can be open or closed. The closed cell content examination was carried out to evaluate the distribution of closed or open cells in VO-based PU foams. In this measurement, an ultra pycnometer (Ultrafoam 1000) shown in **Figure 17**, was used to measure closed-cell content according to the ASTM D2856. This instrument consists of two interconnected parts: a chamber and a pressure-temperature sensor. First, the volume of the empty chamber was determined by opening the valve that allowed nitrogen gas to enter the chamber. The chamber was then filled with a cylindrical sample of known dimensions and mass to determine closed-cell content.



Figure 17. Digital photo of Ultrapycometer (Ultrafoam 1000).

2.6.3. Compressive Strength

The compressive strength of the foams was measured using a Q-Test 2-tensile machine (MTS, USA), as shown in **Figure 18**, following ASTM 1621. Compressive strength, defined as the maximum force created over the surface of a material, was determined by compressing foam between parallel plates with a continuously applied load. To measure the compressive strength of PU foams, the cylindrical samples were placed on a larger surface between two parallel compression plates. Blue Hill software was used to measure the yield break and strain at 10%, and a strain rate of 3 cm/min from the top.

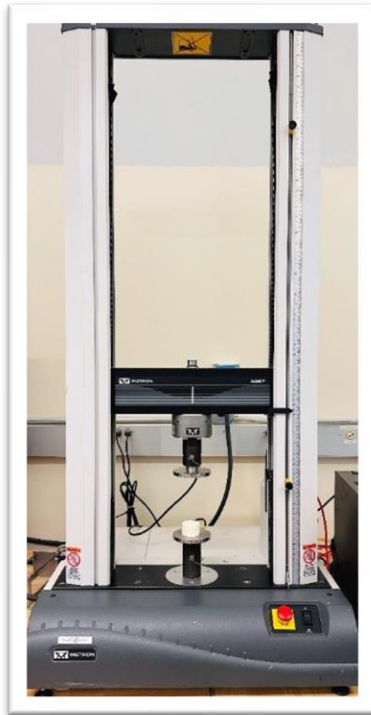


Figure 18. Digital photo of Q test 2-tensile machine.

2.6.4. Scanning Electron Microscope

The cell morphology of the foams was studied using a scanning electron microscope (SEM). Cellular structure of the PU foams was examined using SEM images in terms of pore shape, pore size, and pore distribution. A two-step procedure was used to capture images of the foam samples. Initially, the top part of the foam was cut into cubic forms with 0.5 cm side dimensions. These samples were then placed in a magnetron sputtering device to get a thin coating of gold on their surfaces. **Figure 19** shows a gold sputtering instrument (Kurt J. Lesker Company) that was used before taking images to increase image quality (conductive coating prevents charge buildup). Following the application of a thin conductive gold coating to the top of the polyurethane foam samples, images were acquired using a Thermo Scientific Phenom Pure desktop SEM obtained from the Sioux company in the Netherlands.



Figure 19. Digital photo of gold layer sputtering (left), thermo scientific phenom (right).

2.6.5. Horizontal Burning Test

The ASTM D4986-98 standard was used to study the horizontal burning test of RPUFs. Rectangular specimens of 150 mm in length, 50 mm in breadth, and 12.5 mm in thickness were made for the burning test. Each sample's weight was recorded, and each foam specimen was then exposed to a direct flame for 10 seconds. After the exposure, self-extinguishing time and weight loss were measured. The following experiment was carried out in a fume hood that had good ventilation to eliminate fumes created during decomposition, as shown in **Figure 20**.



Figure 20. Digital photo of horizontal burning test setup.

2.6.6. Thermogravimetric Analysis

Thermogravimetric Analysis (TGA) was used to investigate the stability of bio-based polyurethane foams under increasing temperatures of up to 600 °C. The change in the initial weight of the foams with temperature variations was measured. The thermal behavior and decomposition of RPUFs were investigated using the TA instrument (TGA Q-500), as shown in **Figure 21**. A sample of around 5-8 mg was placed on an aluminum pan and heated at a ramp rate of 10 °C/min, achieving temperatures of up to 600 °C in a nitrogen environment.

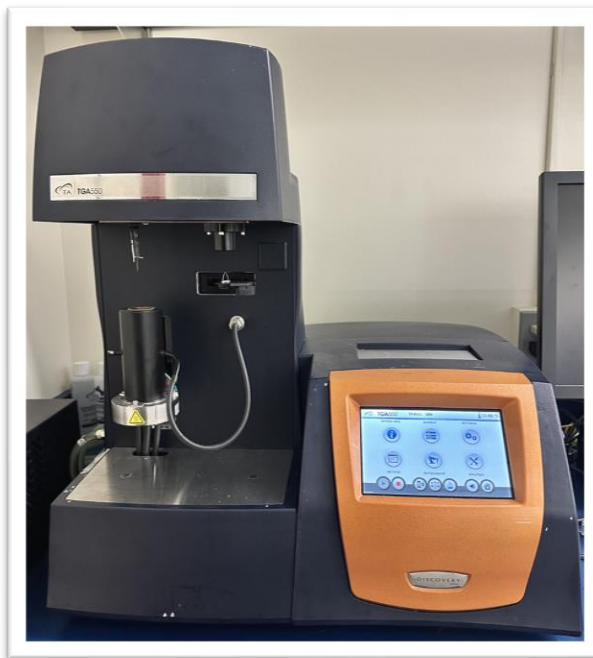


Figure 21. Digital photo of thermogravimetric analysis instrument.

CHAPTER III

RESULTS AND DISCUSSIONS

3.1. Properties of VO, EVO, and VP

3.1.1. Iodine Value

The Hanus approach was used to determine the iodine value and the degree of unsaturation, the amount of double bonds, in VO. The iodine value of VO was 126.37 g I₂/100 g oil, which means that 0.49 molecules of double bonds were present in 100 g of the VO sample. Following the epoxidation and ring-opening processes, the measured iodine values for the epoxide and polyol were 3.01 g I₂/100 g and 1.63 g I₂/100 g, respectively. This shows that the double bonds in VO were converted into a more reactive and useful form (hydroxyl group) to produce rigid polyurethane foam.

3.1.2. Epoxide Number

The percentage of oxirane value indicates how many epoxide groups exist in a material. In this study, the epoxide number was tested following the epoxidation reaction of VO, and it was 7.10 %. This reaction was carried out with hydrogen peroxide and acetic acid in the presence of a catalyst. After the ring-opening process, the epoxide number for polyol was tested and found to be 0.2%, confirming the epoxy ring's conversion into hydroxyl groups.

3.1.3. Hydroxyl Value

One of the most important polyol parameters is the hydroxyl number, which regulates isocyanate reactivity and the amount needed to produce polyurethane. In this study, the determined OH value for VP was 187.01 mg KOH/g.

3.1.4. Acid Value

The VO-derived polyurethane foams were created using an amine-based catalyst. As a result, having a high acid value for the vegetable oil polyol minimizes foaming since the acidic polyol and amine-based catalysts will not react as expected. So, the acid values for all three oils, VO, epoxide oil, and vegetable oil polyol, were determined and found to be 0.68 mg KOH/g, 0.86 mg KOH/g, and 0.99 mg KOH/g, respectively.

3.1.5. Viscosity

Viscosity is a measure of a material's resistance to flow. The measured viscosity of the VO was 0.02 Pa.s, the epoxide VO was 0.07 Pa.s, and the vegetable oil polyol was 1.48 Pa.s. The viscosity measurement additionally suggests that the molecular weight increased following the modification of polyol from the oil.

Table 3. Characterization of vegetable oil, epoxidized vegetable oil, and vegetable oil polyol.

Test names	Unit	Vegetable oil	Epoxidized vegetable oil	Vegetable oil polyol
Iodine value	g I ₂ /100g	126.37	3.01	1.63
Epoxy-oxirane oxygen content	%	-	7.10	0.23
Hydroxyl number	mg KOH/g	-	-	187.01
Acid value	mg KOH/g	0.68	0.86	0.99
Viscosity @25°C	Pa.s	0.02	0.07	1.48

3.1.6. Fourier Transform Infrared Spectroscopy

FTIR is an effective analytical method for determining the molecular bonding in a material. This approach was used to effectively validate the synthesis of polyol and epoxide from VO. A typical sign of unsaturation in the FTIR spectra of different fats and VOs is detected at 2989-3029 cm⁻¹ [64]. **Figure 22** shows the FTIR spectra of VO, EVO, and VP. As shown in the FTIR spectra of VO, based on the stretching vibration from the =C-H, the peak that was noticed around the wavenumber at 3011 cm⁻¹ denoted the presence of a carbon-carbon (C=C) double bond [65][66]. After the epoxidation process, that peak disappeared, and a new peak was observed around 823 cm⁻¹. This new peak was related to

the bending of the epoxy group in the C-O-C ring in the EVO which indicated the successful modification of epoxidized oil [67]. The peak of the epoxide ring (C-O-C) vanished after the ring-opening process, and in its place, a new broad peak appeared at 3458 cm^{-1} , which represented the stretching vibration of the hydroxyl group (O-H) in the VO [68][16]. This FTIR peak verifies the formulation of vegetable oil-based polyol and provides evidence for future synthesis to produce VP-based foams.

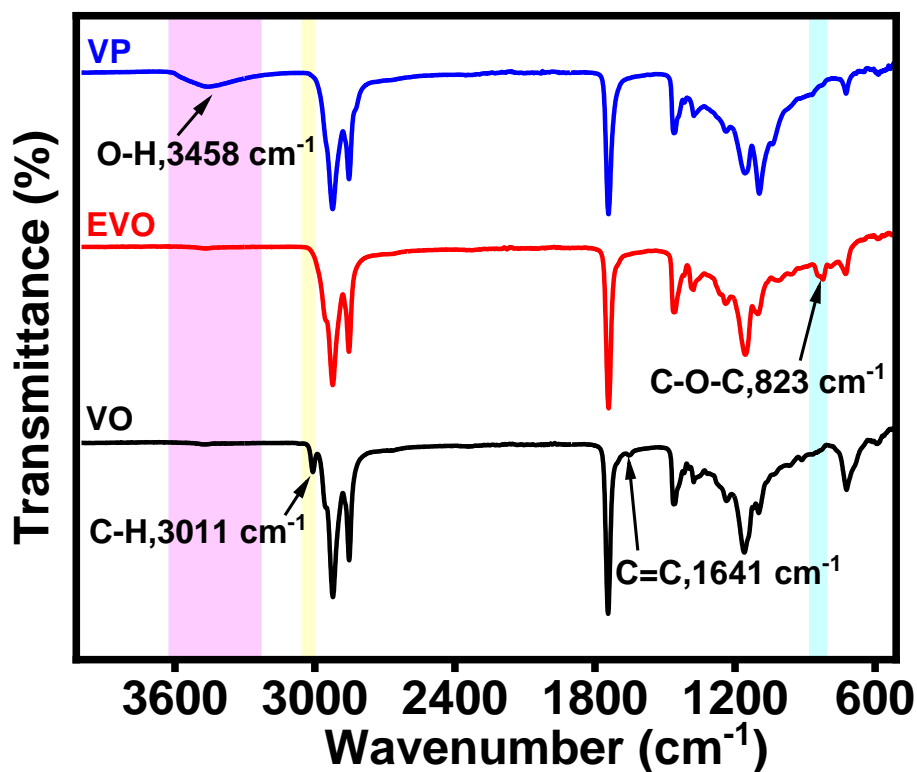


Figure 22. FTIR spectra of vegetable oil (VO), epoxidized vegetable oil (EVO), and vegetable oil polyol (VP).

3.1.7. Gel Permeation Chromatography

GPC is generally used for determining the molecular weight distribution of polymers. It is known that larger molecules pass through the column faster because they avoid getting stuck in the pores of the polymeric beads that compose the stationary phase. On the other hand, smaller molecules take longer to pass through the column as their movement becomes hindered because of the pores in the stationary phase. Based on that, as per the GPC curves, the retention time of polyurethanes (32.17 min) is the shortest when compared to the others, which was likely due to the introduction of hydroxyl groups into its structure after the epoxidation process. The retention time for EVO and VO is 32.19 and 32.41 minutes, respectively (**Figure 23**).

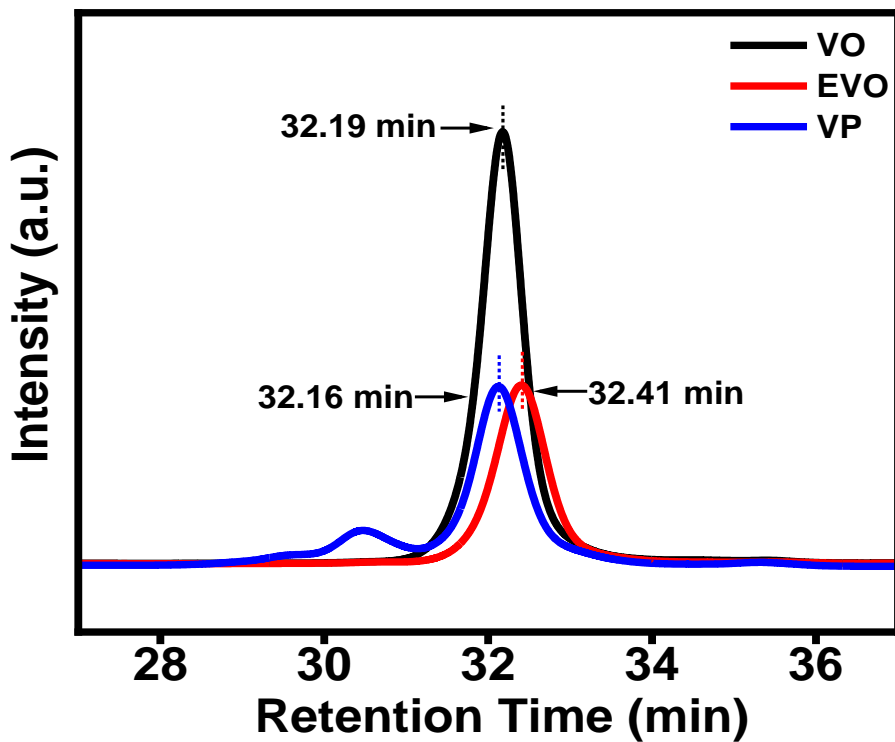


Figure 23. GPC of vegetable oil (VO), epoxidized vegetable oil (EVO), and vegetable oil polyol (VP).

The molecular weight of EVO was lower than that of VP because it had a faster elution time, indicating that the molecular weight of polyol rose during the procedure. However, it could be noticeable on the chromatogram for the VP that there was a second peak that appeared at a shorter elution time. That peak could be attributed to the formation of a dimer or oligomer during the ring-opening reaction that led to the formation of a polyol with a relatively larger molecular weight than the predominant compound [16]. EVO is polar, whereas VO is nonpolar. The polar nature of the silica gel supplied to the GPC column may have interacted with EVO (polar-polar interaction), resulting in slower EVO elution.

3.2. Properties of Flame-Retardant

3.2.1. Fourier Transform Infrared Spectroscopy of DPPMA FR

DPPMA's chemical structure was validated using FTIR. The FTIR spectra of DPPA, MA, and DPPMA are shown in **Figure 24**. In the MA spectra, the two peaks at 3468 cm^{-1} and 3417 cm^{-1} come from the stretching vibration of $-\text{NH}_2$ as well as the peak at 3329 cm^{-1} and 3128 cm^{-1} which were attributed to N-H bonds according to the FTIR spectra of the starting materials [69]. Also, the small peak at 1646 cm^{-1} was assigned to N-H bonds [70]. In the DPPA spectra, the small peak at 2614 cm^{-1} was attributable to $\text{O}=\text{P}-\text{OH}$ groups [60,71]. After the reaction between DPPA and MA, the peak of $-\text{NH}_3^+$ was observed at 3112 cm^{-1} and 1609 cm^{-1} in the final product, DPPMA. The peak seen in MA at 1646 cm^{-1} and

3329 cm^{-1} remained in DPPMA after the synthesis of DPPA and MA, which was assigned to N-H bonding.

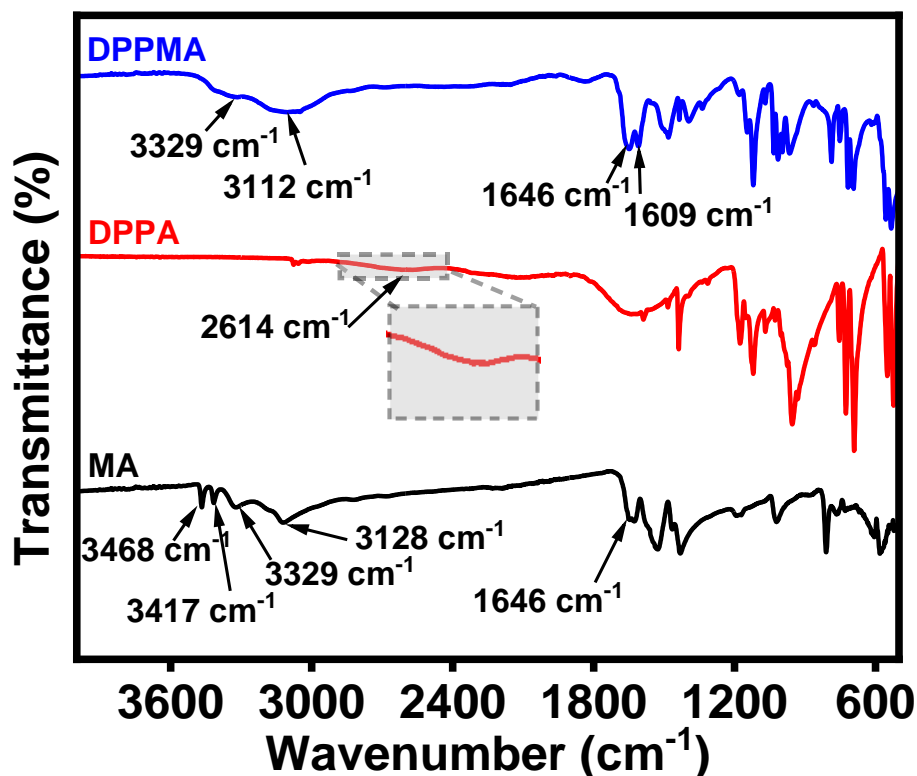


Figure 24. FT-IR of MA, DPPA and DPPMA.

3.2.2. ^1H Nuclear Magnetic Resonance

The ^1H NMR spectroscopy was also performed for the starting materials and the synthesized FRs to investigate the successful modification of DPPMA which is displayed in **Figure 25**. Apart from the peaks of the solvent (DMSO D6) and moisture, the ^1H NMR for MA displayed one peak at 5.9 ppm assigned for hydrogen atoms bonded with nitrogen in an aromatic ring [72]. Two noticeable peaks were identified in the DPPA spectra at 7.3

and 7.6 ppm, which were attributed to the hydrogen atoms from the aromatic ring of DPPA. However, after the reaction between DPPA and MA, a new peak at 7.4 ppm was found, which corresponded to the hydrogen from the $-NH_2$ from the DPPMA [60].

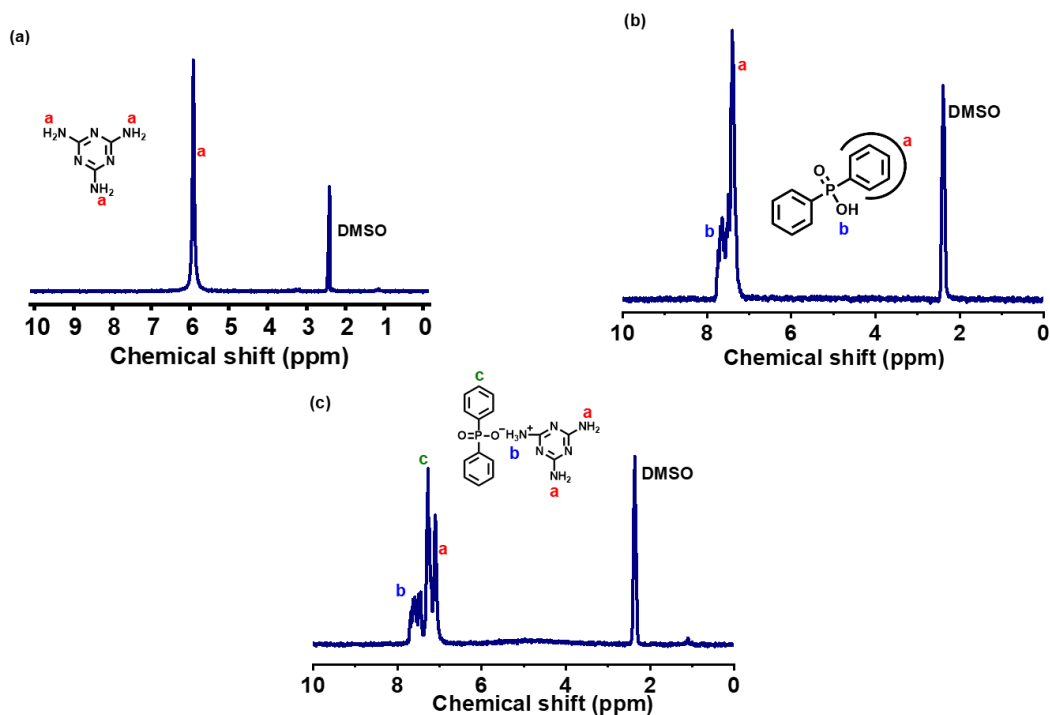


Figure 25. ^1H NMR of MA, DPPA and DPPMA.

3.3. Properties of the VO-Based RPUFs

3.3.1. Closed Cell Content

The ratio of open and closed cells significantly impacts the usefulness of RPUFs. It also evaluates thermal insulation and water absorption qualities [73]. RPUFs with a high closed-cell content offer superior insulation. A foam with a closed cell structure presents encapsulated air pockets that are usually not interconnected with each other. Such

morphology tends to decrease the conductivity of heat and the permeation of oxygen within the foam. The RPUFs with the MA FR showed around 88% to 90% of closed cell content as shown in **Figure 26**. This means less air diffusion occurred in foams after increasing the amount of MA. However, it was observed that foams with DPPMA and DMMP showed a decrement in closed cell content with an increasing amount of FR. Despite that, all RPUFs displayed a closed cell content of more than 60% which meets the requirements for industrial standards.

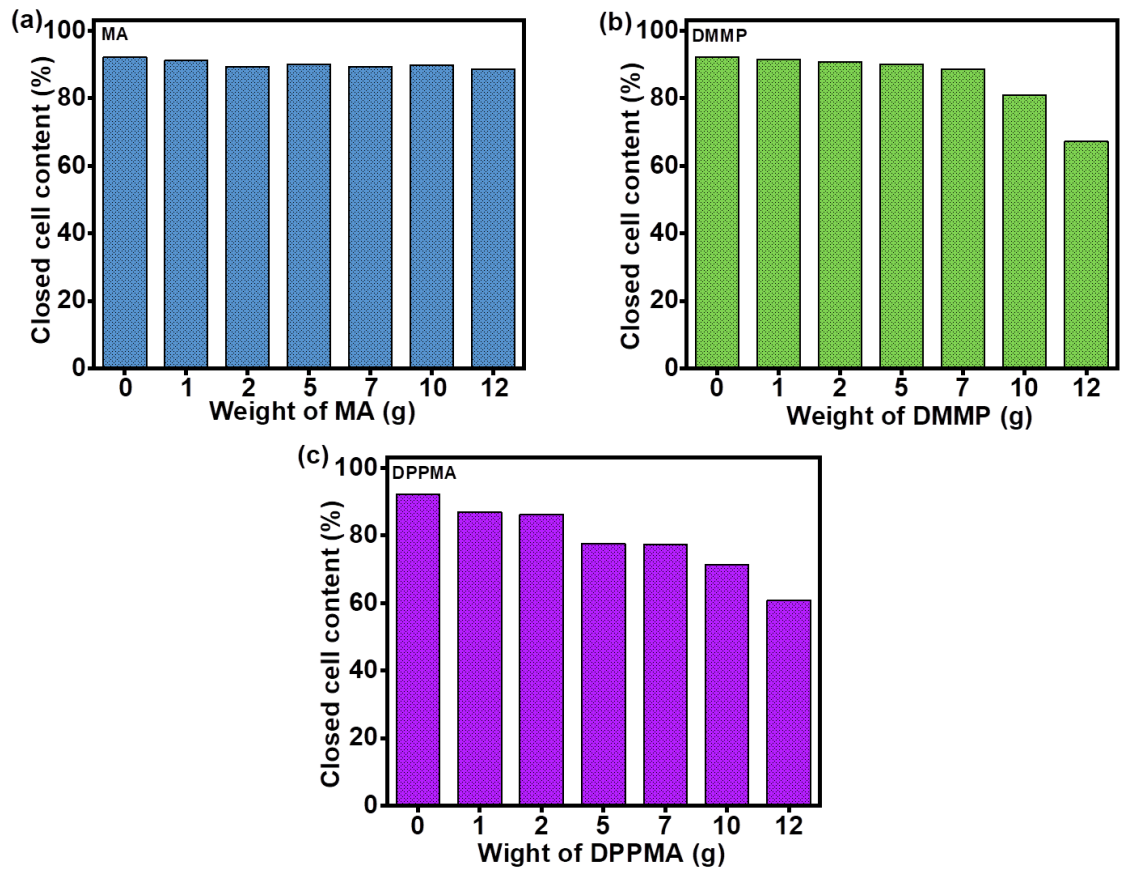


Figure 26. Closed-cell content of the obtained RPUFs with different weights of (a) MA, (b) DMMP, and (c) DPPMA as FRs.

3.3.2. Apparent Density

The density is an important physical property that can point to some of the applications for a given material. Based on that, the density of the RPUFs was measured and displayed in the bar graph as shown in **Figure 27**. After the addition of MA or DMMP FRs to the RPUFs, the density increased in proportion to the wt.% of FRs. In this sense, the densities of most of the foams ranged from 21 to 44 kg/m³, which followed the commercially available RPUFs range of 20-50 kg/m³ [74]. However, higher DMMP loadings in the foam caused some shrinkage due to the acidity of DMMP which can react with the tertiary amine that was used as catalysts for the reaction between isocyanate and water that leads to the evolution of CO₂ within the foam. In this sense, the evolution of CO₂ occurred at a lower rate since the alkaline tertiary amine could be partially consumed by the acidic DMMP, which increased the density of the RPUF as the sample DMMP-12 g presented the highest value of 79.17 kg/m³. Such an effect of an increase in density upon the addition of P-based FRs has been observed in previous studies [75]. In the case of DPPMA, there was an increase in density up to DPPMA-5 g. However, the continued addition of DPPMA to the RPUFs resulted in a reduction in height. To overcome this, catalyst, blowing agent, and isocyanate amounts were increased for the consecutive RPUFs, DPPMA-7 g, DPPMA-10 g, and DPPMA-12 g. This change in formulation increased the height of the RPUFs due to the production of CO₂ gas, making the gas phase appear more prominently than the solid phase, resulting in a decrease in their densities because there was a small increase in overall weight for a larger increase in volume, lowering the density [76,77].

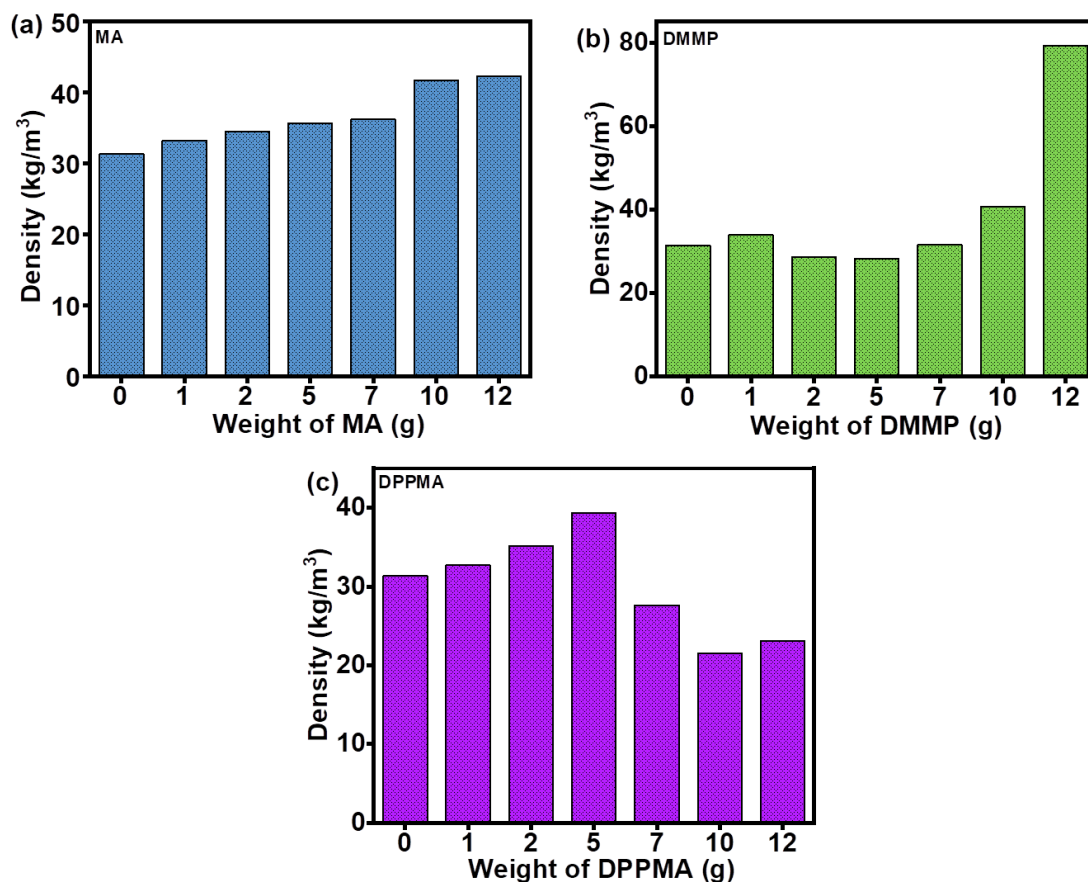


Figure 27. The apparent density of the obtained RPUFs with different weights of (a) MA, (b) DMMP, and (c) DPPMA as FRs.

3.3.3. Compressive Strength

The mechanical strength of the RPUFs is affected by their density, cell size, and interactions with other fillers. Based on that, the compressive strength of the RPUFs containing increasing amounts of MA, DPPA, or DPPMA is presented in **Figure 28**. It was observed that the control sample presented a compressive strength of around 200 kPa. For the case of the RPUFs containing increasing concentrations of MA, it was observed that a

fluctuation in the values of compressive strength was as MA-2 g had the lowest value around 180 kPa whereas MA-10 g had the maximum around 220 kPa. Despite the fluctuation in the compressive strength, the obtained values were relatively similar. Based on that, the slight improvement in mechanical strength could be attributed to an attractive intermolecular interaction between MA and the hard segments of the RPUFs, which could, perhaps, decrease the microphase separation that could be the reason for the minor increase in compression strength.

For the case of the RPUFs containing increasing concentrations of DMMP the highest compression was observed for DMMP-1 g which was around 225 kPa. However, upon the increase of DMMP concentrations, there was a decrease in compressive strength for the RPUFs DMMP-2 g and DMMP-5 g which were around 170 and 160 kPa, respectively. However, upon further increase in the concentration of DMMP, there was also an increase in compressive strength as the values for DMMP-7 g, DMMP-10 g, and DMMP-12 g were around 175, 180, and 210 kPa, respectively. The increase in compressive strength could be attributed to the decrease in the RPUFs' expansion which led to an increase in density that could have caused their mechanical compression strength to increase [42].

The RPUFs containing increasing amounts of DPPMA had a continuous decrease in compressive strength as it went from 200 kPa (control sample) to the lowest of 48 kPa for DPPMA-10 g the optimal value was obtained for DPPMA-5 g with a value of around 178 kPa. However, a continuous decrease in the compressive strength was observed upon the addition of higher amounts of DPPMA. This might be because of the increased cell size caused by the addition of FR to foams.

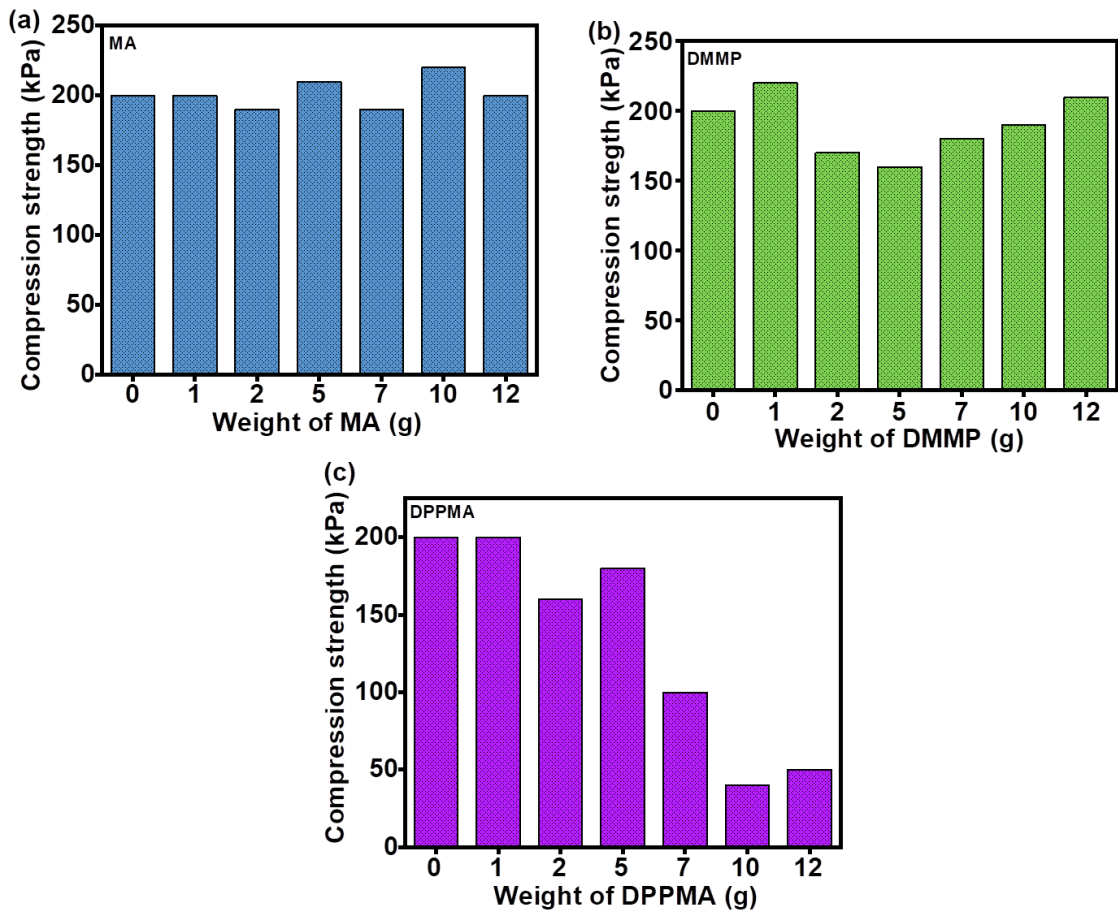


Figure 28. Compressive strength of RPUFs with different weights of (a) MA, (b) DMMP, and (c) DPPMA FRs.

3.3.4. Cellular Morphology

A scanning electron microscope was used to examine the microstructure and morphology including average cell size, uniformity, and cell distribution of RPUFs containing MA, DMMP, and DPPMA. It is believed that the cell structure of RPUF has a significant impact on its mechanical characteristics. In general, it could be observed that all the foams had their cellular structure preserved suggesting that the addition of larger

amounts of FRs did not disrupt the RPUF morphology. Further on, in the morphology of the MA-containing RPUFs, it was observed that the addition of MA to the RPUF's matrix promoted a small variation in the cell size, as it ranged from around 160 to 195 μm . Such a small variation could suggest that MA had a better interaction with the RPUFs (**Figure 29**). However, when the concentration of DMMP in the foam increased, also increased the size and irregularity of the cells shown in **Figure 30**. Such an effect could be partially correlated with the response on the compressive strength as an increase in cell size led to a decrease in cell number. As a result, the RPUF matrix would have fewer cells to endure mechanical stress over its surface [42]. However, further addition of DMMP promoted a fast curing of the foam which led to a decrease in cell size as well as more irregularities in the morphology. In this sense, the decrease in cell size could have played a role in the slight increase in the compressive strength of the foams. In the case of DPPMA, it could be noticed a more drastic increase in the cell size of foams which could range from 300 to around 600 μm illustrated in **Figure 31**. Such variation could justify the decrease in the compressive strength as the larger cells diminished the mechanical support in the overall structure of foam which made them mechanically weaker [60,77].

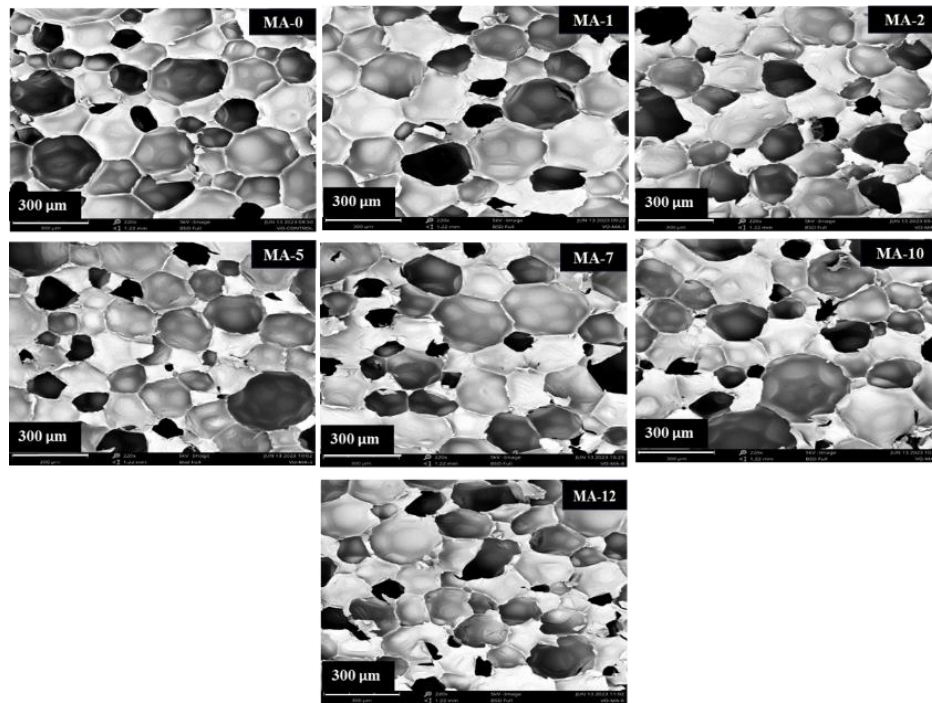


Figure 29. SEM images for RPUFs with varying amounts of MA.

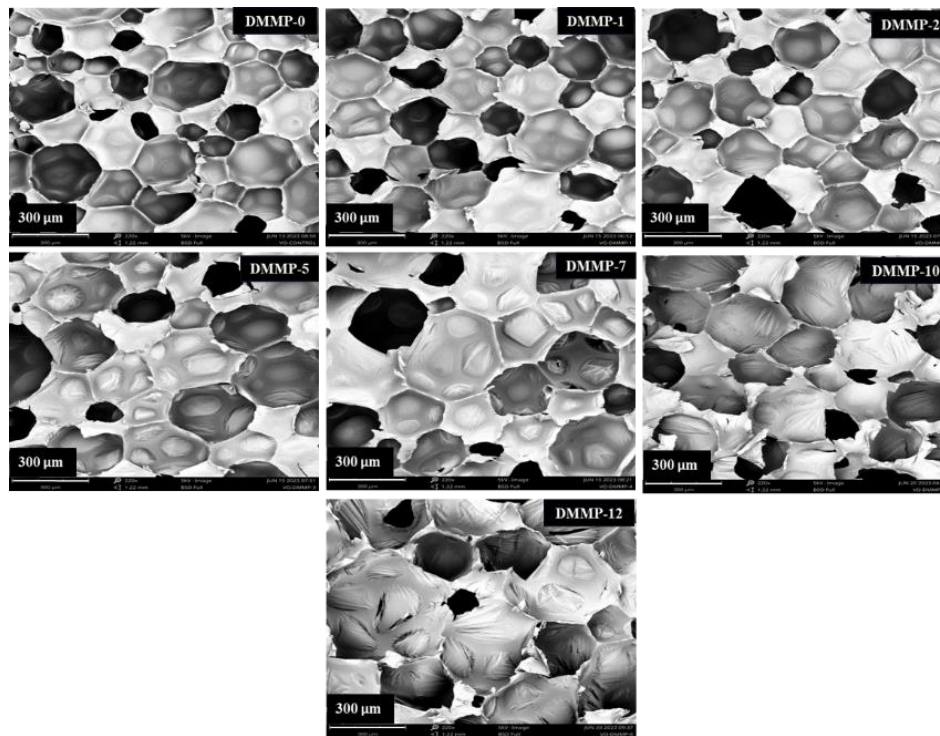


Figure 30. SEM images for RPUFs with varying amounts of DMMP.

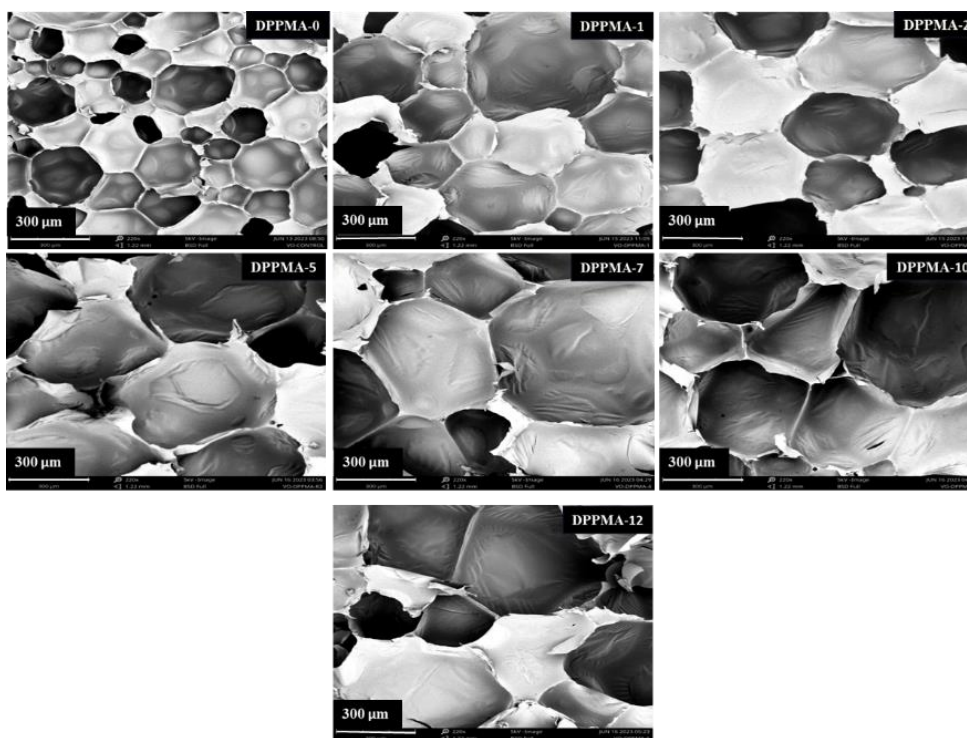


Figure 31. SEM images for RPUFs with varying amounts of DPPMA.

3.3.5. Thermogravimetric Analysis

TGA and DTGA results were also used to understand the thermal characteristics of foam containing increasing amounts of MA, DMMP, and DPPMA. Based on that, the TGA and DTGA for the RPUFs containing increasing amounts of MA are shown in **Figure 32**. Considering the control sample two thermal transitions could be observed in all the foams the one that occurred at around 250 °C could be attributed to the decomposition of the rigid segments into polyols, amines, and gaseous species and the other occurred at around 450 °C which could be attributed to the decomposition of soft segments from the aliphatic segments of the polymeric matrix [60,78,79].

It was observed on the DTGA plot for RPUFs MA that there were four thermal decompositions. Foams decomposed between 290-320 °C and 450 °C, resulting in the breakdown of urethane linkages and hard segments, as well as disruption of soft segments in RPUFs [78,80]. The first and third thermal decompositions are related to the thermal behavior of MA. The first transition can be linked to MA's endothermic breakdown at temperatures ranging from 290 to 320 °C. The major decomposition was observed at around 320 °C which is related to the breakdown of urethane linkage and hard segments of the RPUFs. The fourth thermal transition occurred at around 450 °C and was connected with the synthesis of oligomeric derivatives of MA [81,82].

The TGA and DTGA behavior of the RPUFs containing increasing amounts of DMMP are presented in **Figure 33**. From that, an early loss of weight could be observed at an onset temperature of 150 °C which was associated with the decomposition of DMMP [58]. Further, the second decomposition at around 300 °C was attributed to the decomposition of the hard segments of the RPUFs. However, there could be a slight shift towards higher temperature as the concentration of DMMP increases in the RPUFs. Such an effect suggested a slight increase in thermal stability for that transition. Lastly, the decomposition at 450 °C was attributed to the decomposition of the soft segments in RPUFs.

The TGA and DTGA for the RPUFs containing increasing amounts of DPPMA are shown in **Figure 34**. There were two major thermal decompositions which were likely attributed to the decomposition of the hard segments of the RPUFs around 325 °C and the second decomposition related to the decomposition of soft segments at 450 °C [83]. Further

on that, it could be noted a slight shift in thermal decomposition towards higher temperatures which implied an improvement in thermal stability after the addition of DPPMA. Along with that, there was also a larger residue content percentage during all thermal transitions when compared to the other forms. In this sense, a favorable aspect of DPPMA was that the decomposition temperatures of FR and the RPUFs were within a close range. Such conditions allow for the FR to decompose at the same temperature as the RPUFs leading to an optimized FR action [51].

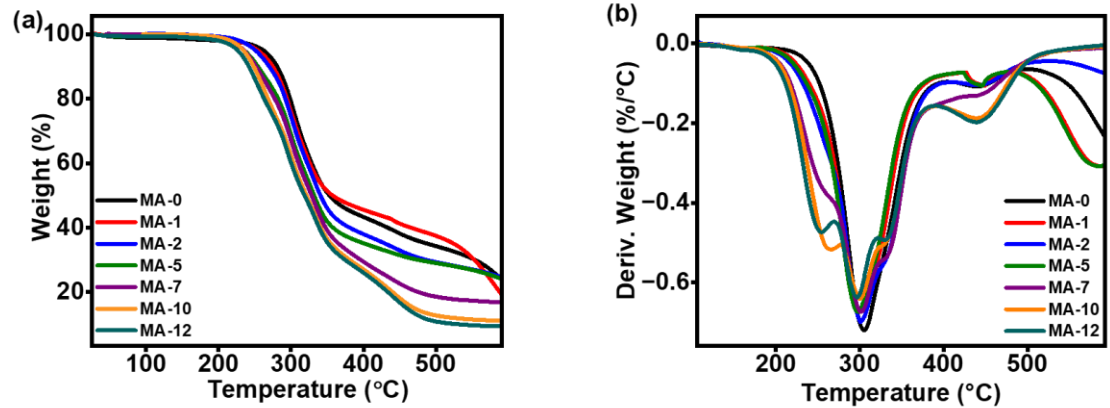


Figure 32. RPUFs with varying amounts of MA (a) TGA, (b) DTGA.

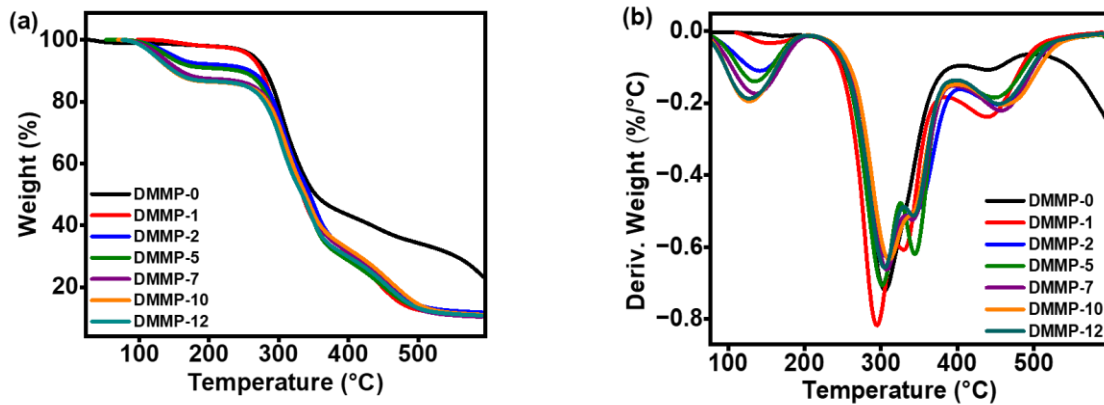


Figure 33. RPUFs with varying amounts of DMMP (a) TGA, (b) DTGA.

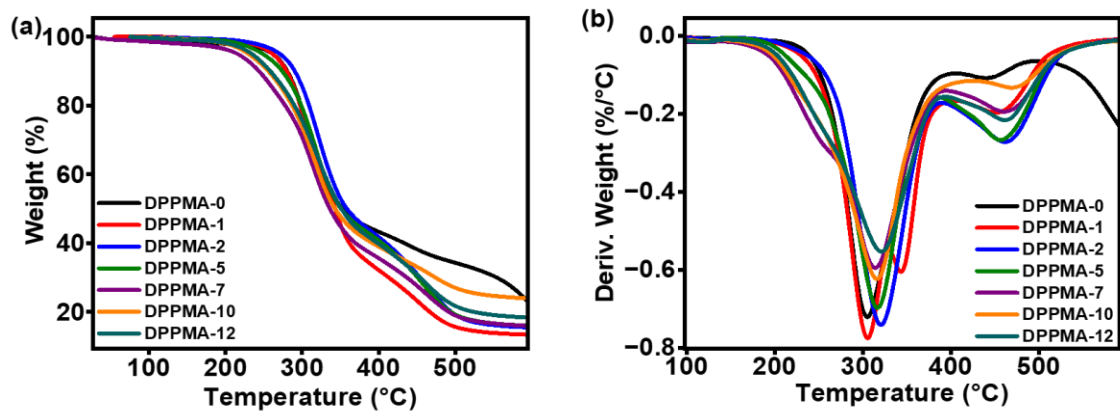


Figure 34. RPUFs with varying amounts of DPPMA (a) TGA, (b) DTGA.

3.3.6. Horizontal Burning Test

The horizontal burning test was performed to analyze the fire-quenching capabilities of the RPUF containing MA, DMMP, and DPPMA. The foams were placed horizontally and subjected to a continuous flame for 10 seconds. Afterward, the flame was removed, and the time required for the foam to extinguish the fire, as well as its weight loss, was recorded [84]. The control sample showed the longest burning time of 62 seconds as well as the highest weight loss of 56%. The fastest response to fire quenching was observed for the RPUF DMMP-12 g which presented a burning time of around 1 second and weight loss of 5.1%. For the case of RPUFs containing MA the sample MA-12 g presented a burning time of 6 seconds and a weight loss of 7.05%. However, the DPPMA-7 g had a burning time of 18 seconds along with a weight loss of 20%. Despite the relatively higher burning time and weight loss of DPPMA in comparison to MA and DMMP, it is worth noting that the addition of DPPMA could be added in larger amounts without

promoting shrinkage of the foams as was the case for DMMP. **Figure 35** shows the weight loss and burning time in RPUFs with three different FRs.

There have been a considerable number of studies that described the FR mechanism for several materials. In this sense, MA is a material that can act on both solid and gas phases during the combustion process. It undergoes a progressive endothermic condensation that leads to the release of ammonia that can dilute combustible gases such as oxygen and or flammable species that are formed during combustion. As that process occurs, MA can also form a thermostable char layer composed of polymerized products of its combustion which are known as melon, melam, and melem. These compounds can protect the polyurethane foams underneath the layer from oxygen and reactive species [51,81].

DMMP is also known to be active in the condensed and vapor phases. To begin with, the thermal breakdown of DMMP produces phosphoric acid, which rapidly condenses to form phosphorous structures and release water. This dehydration results in the creation of carbocation and carbon-carbon double bonds. At high temperatures, this results in the production of a carbonized crosslinked structure on the PU foam as a char layer, which protects the foam from the flame, prevents the generation of new free radicals, and limits the passage of oxygen, resulting in a decrease in combustion. Second, the DMMP volatilizes into the gas phase, forming PO_2^\bullet , PO^\bullet [27,51].

In the case of DPPMA, it could be proposed that it decomposes into phosphorous and benzene gaseous derivatives, derived from DPPA, which further produce pyrophosphoric acid in the condensed phase. Along with that, it releases ammonia, derived from the MA, during the heating process, forming the condensates melon, melem, and

melan and generating the char layer. The condensation product is also crosslinked with diphenyl phosphinic acid to generate phosphocarbonaceous structures that prevent the foam from burning [60]. **Figures 36, 37, and 38** show the picture of RPUFs before and after the horizontal burning test with different FRs.

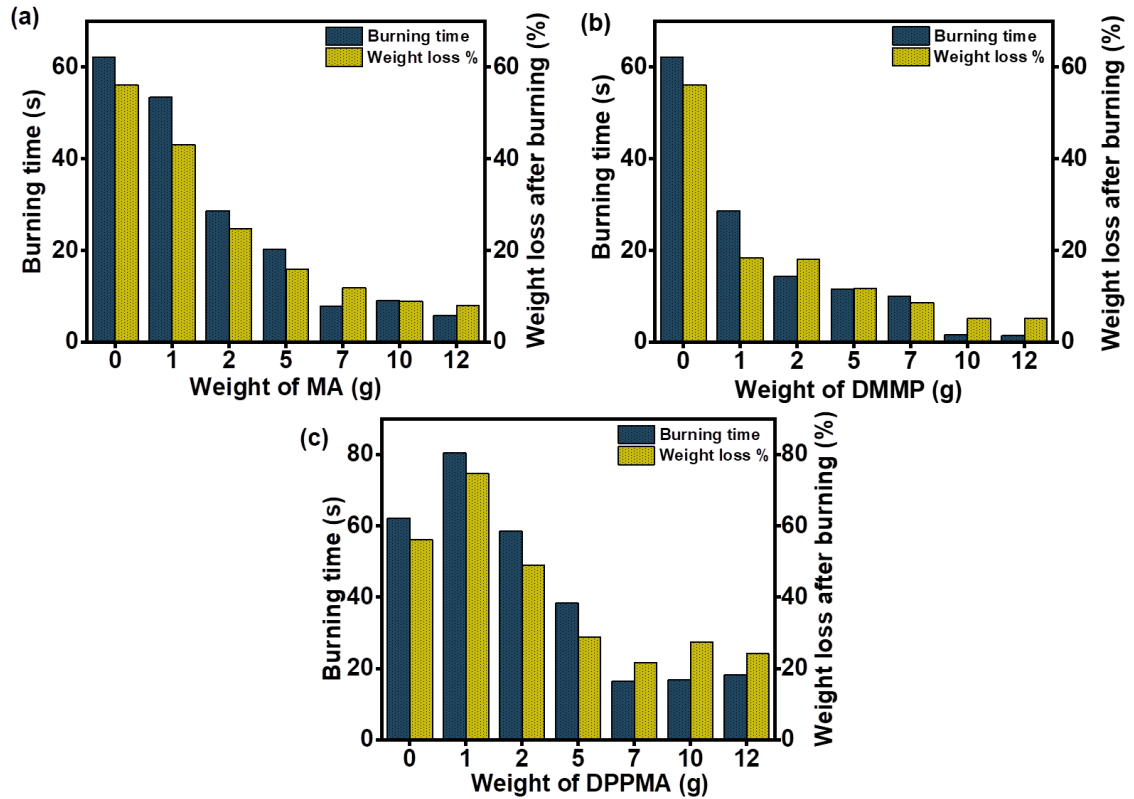


Figure 35. Comparisons of burning time and weight loss percent of RPUFs with different weights of (a) MA, (b) DMMP, and (c) DPPMA.

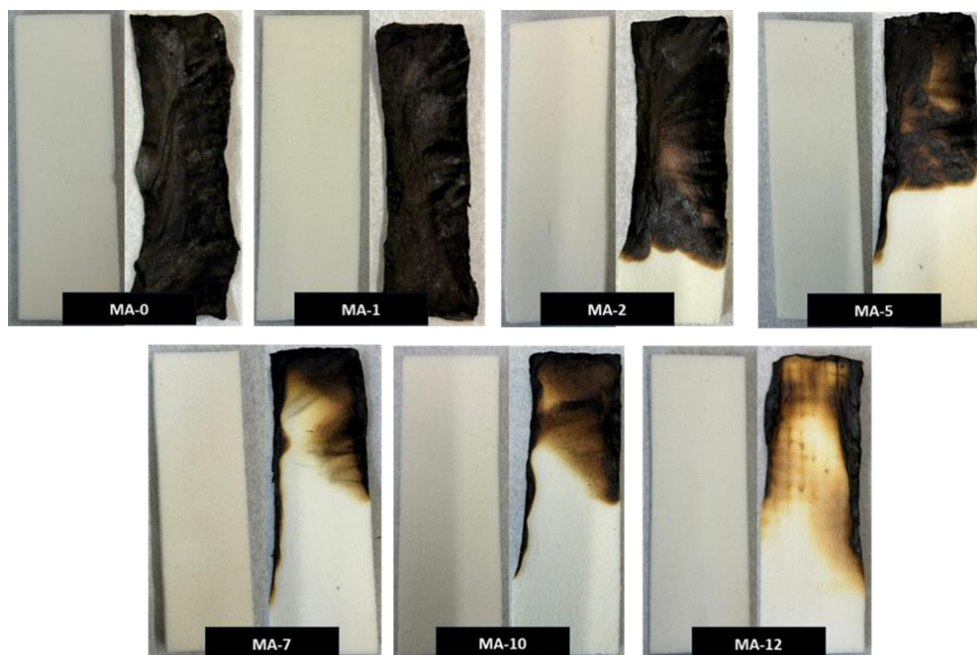


Figure 36. Digital photographs of RPUFs before and after the horizontal burning test with different concentrations of MA.

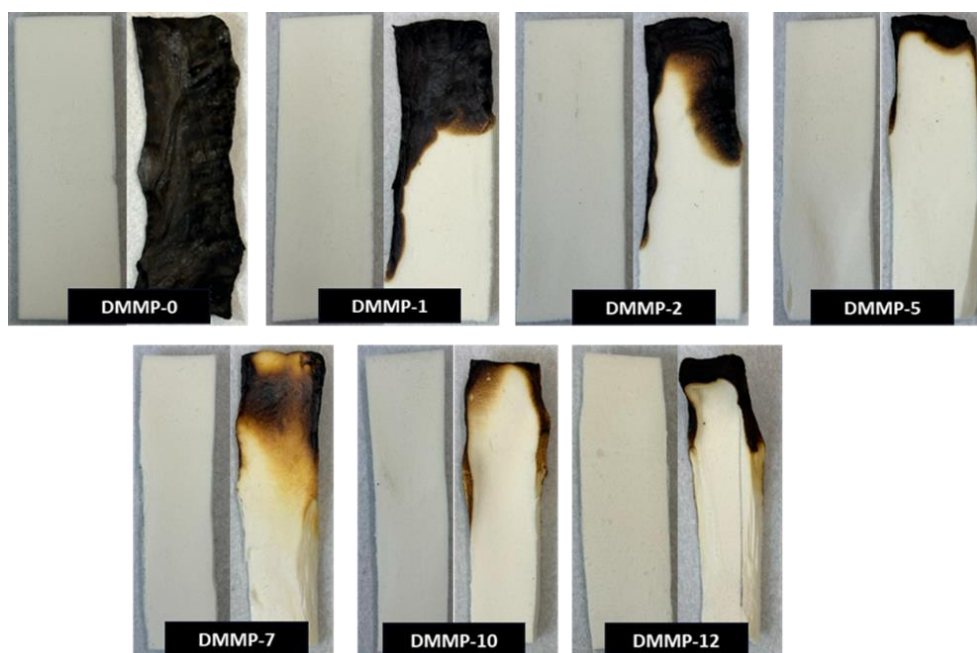


Figure 37. Digital photographs of RPUFs before and after the horizontal burning test with different concentrations of DMMP.

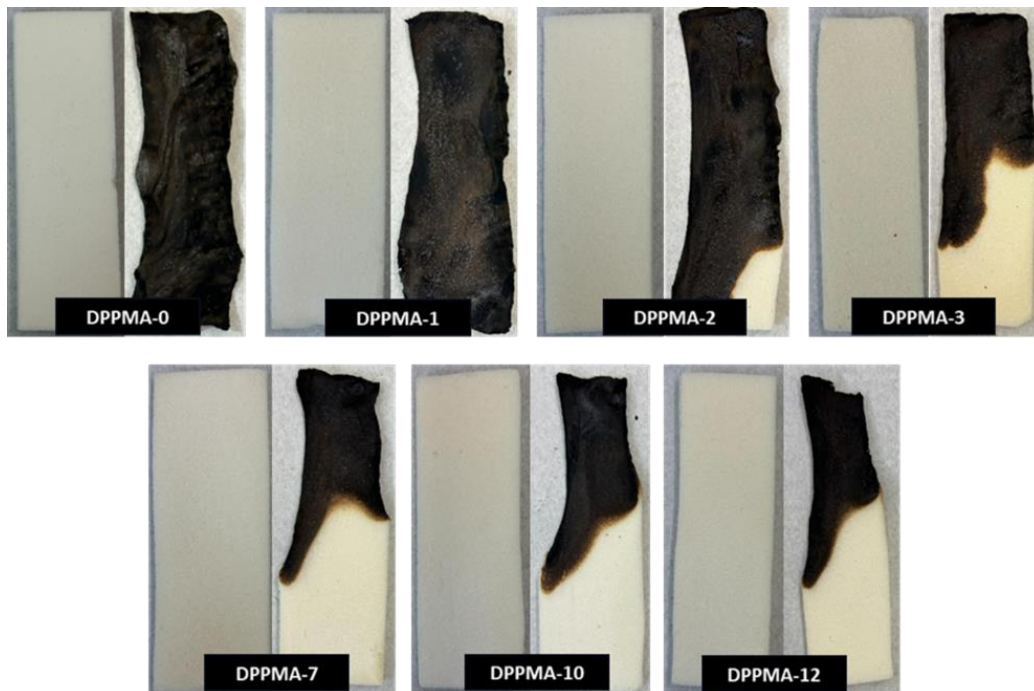


Figure 38. Digital photographs of RPUFs before and after the horizontal burning test with different concentrations of DPPMA.

CHAPTER IV

CONCLUSIONS

In this work, VP was successfully synthesized using a two-step process of epoxidation and ring-opening reactions. The polyol was later used to make RPUFs. During the making of the RPUFs, three FRs: MA, DMMP, and DPPMA were added separately. Most foam densities remained within the industry-standard range of 21 to 44 kg/m³. Most of the foams containing MA maintained their closed cell content above 88%. However, foams containing DMMP and DPPMA presented lower closed cell content to around 67% and 60% after additions of 12 grams of FRs. In terms of compression strength, there was a variation in the values as the control sample presented around compression strength 210 kPa. After the incorporation of increasing amount of MA into foams the compressive strength remained between 190-220 kPa. For the RPUFs containing DMMP, there was a slightly higher variation in compressive strength values with an increase to 225 kPa followed by a fluctuation of values that were like those of the control sample. In the case of DPPMA, there was a continuous decrease in compression strength upon increasing its concentration in the RPUFs with the highest and lowest of around 178 and 40 kPa. The burning test revealed that the flammability considerably decreased even with the addition of a smaller amount of MA, DMMP, and DPPMA. For example, the incorporation of 7 g

of MA, DMMP, and DPPMA showed 7.9 seconds, 10 seconds, and 16.4 seconds, and 11.92%, 8.59%, and 21.68% burning time and weight loss, respectively.

REFERENCES

- [1] A. Sionkowska, Current research on the blends of natural and synthetic polymers as new biomaterials: Review, *Prog. Polym. Sci.* 36 (2011) 1254–1276.
- [2] A. Tenorio-Alfonso, M.C. Sánchez, J.M. Franco, A Review of the Sustainable Approaches in the Production of Bio-based Polyurethanes and Their Applications in the Adhesive Field, *J. Polym. Environ.* (2020) 1–26.
- [3] K. Duncan, Connecting with the creator, *World Lit. Today.* 87 (2013) 82–87.
- [4] P.M. Size, M.D. Di-isocyanate, B. Product, B. Application, S. Forecasts, *Polyurethane Market Size & Trends Market Concentration & Characteristics*, (2024) 1–12.
- [5] P. Schara, A.M. Cristadoro, R.P. Sijbesma, Ž. Tomović, Solvent-Free Synthesis of Acetal-Containing Polyols for Use in Recyclable Polyurethanes, *Macromolecules.* 56 (2023) 8866–8877.
- [6] U. Šebenik, M. Krajnc, Influence of the soft segment length and content on the synthesis and properties of isocyanate-terminated urethane prepolymers, *Int. J. Adhes. Adhes.* 27 (2007) 527–535.
- [7] R.K. Gupta, P.K. Kahol, eds., *Polyurethane Chemistry: Renewable Polyols and Isocyanates*, 1st ed., American Chemical Society, Washington, DC, 2021.
- [8] R.K. Gupta, ed., *Materials and Chemistry of Flame-Retardant Polyurethanes Volume 1: A Fundamental Approach*, 1st ed., American Chemical Society, Washington, DC, 2021.
- [9] R.K. Gupta, ed., *Materials and Chemistry of Flame-Retardant Polyurethanes Volume 2: Green Flame Retardants*, 1st ed., American Chemical Society, Washington, DC, 2021.
- [10] R.K. Gupta, A.K. Mishra, eds., *Eco-Friendly Waterborne Polyurethanes*, 1st ed., Boca Raton, FL, 2022.
- [11] N. V Gama, A. Ferreira, A. Barros-Timmons, Polyurethane foams: Past, present, and future, *Materials (Basel).* 11 (2018) 1841.
- [12] F.M. de Souza, P.K. Kahol, R.K. Gupta, Introduction to Polyurethane Chemistry, in: R.K. Gupta, P.K. Kahol (Eds.), *Polyurethane Chem. Renew. Polyols Isocyanates*, American Chemical Society, Washington, D.C., 2021: p. 1.
- [13] A.R. Kakroodi, M. Khazabi, K. Maynard, M. Sain, O.S. Kwon, Soy-based polyurethane spray foam insulations for light weight wall panels and their performances under monotonic and static cyclic shear forces, *Ind. Crops Prod.* 74 (2015) 1–8.
- [14] T. Fawzi, L.J. Yu, K.H. Badri, Z. Sajuri, A.A.M. Al-Talib, S.Y. Eh Noum, Sodium hydrogen bicarbonate and water as blowing agent in palm kernel oil based polyol

- polyurethane foam, *Mater. Today Proc.* 39 (2019) 993–998.
- [15] F.M. de Souza, R.K. Gupta, Waterborne Polyurethanes in Sustainability Development, in: *Sustain. Prod. Appl. Waterborne Polyurethanes*, Springer, Cham, 2021: pp. 83–108.
- [16] M.A. Asare, F.M. de Souza, R.K. Gupta, Waste to Resource: Synthesis of Polyurethanes from Waste Cooking Oil, *Ind. Eng. Chem. Res.* 61 (2022) 18400.
- [17] M.A. Asare, F.M. de Souza, R.K. Gupta, Natural Polyurethanes Resources Industries for, in: Ram K. Gupta (Ed.), *Spec. Polym. Fundam. Prop. Appl. Adv.*, CRC Press, Boca Raton, FL, 2023: p. 29.
- [18] S. Bhoyate, M. Ionescu, D. Radojicic, P.K. Kahol, J. Chen, S.R. Mishra, R.K. Gupta, Highly flame-retardant bio-based polyurethanes using novel reactive polyols, *J. Appl. Polym. Sci.* 135 (2018) 46027.
- [19] R.K. Gupta, A.K. Mishra, *Eco-friendly Waterborne Polyurethanes: Synthesis, Properties, and Applications*, CRC Press, Boca Raton, FL, 2022.
- [20] F. M. de Souza, J. Choi, S. Bhoyate, P.K. Kahol, R.K. Gupta, Expendable Graphite as an Efficient Flame-Retardant for Novel Partial Bio-Based Rigid Polyurethane Foams, *C — J. Carbon Res.* 6 (2020) 27.
- [21] S. Bhoyate, M. Ionescu, P.K. Kahol, J. Chen, S.R. Mishra, R.K. Gupta, Highly flame-retardant polyurethane foam based on reactive phosphorus polyol and limonene-based polyol, *J. Appl. Polym. Sci.* 135 (2018) 16–19.
- [22] C. Zhang, S. Bhoyate, M. Ionescu, P.K. Kahol, R.K. Gupta, Highly flame retardant and bio-based rigid polyurethane foams derived from orange peel oil, *Polym. Eng. Sci.* 58 (2018) 2078–2087.
- [23] C. Zhang, S.A. Madbouly, M.R. Kessler, Biobased polyurethanes prepared from different vegetable oils, *ACS Appl. Mater. Interfaces.* 7 (2015) 1226–1233.
- [24] A. Bîrca, O. Gherasim, V. Grumezescu, A.M. Grumezescu, Introduction in thermoplastic and thermosetting polymers, *Mater. Biomed. Eng. Thermoset Thermoplast. Polym.* (2019) 1–28.
- [25] E. Koh, N.K. Kim, J. Shin, Y.W. Kim, Polyurethane microcapsules for self-healing paint coatings, *RSC Adv.* 4 (2014) 16214–16223.
- [26] V. Kanyanta, A. Ivankovic, Mechanical characterisation of polyurethane elastomer for biomedical applications, *J. Mech. Behav. Biomed. Mater.* 3 (2010) 51–62.
- [27] S. Ramanujam, C. Zequine, S. Bhoyate, B. Neria, P. Kahol, R. Gupta, Novel Biobased Polyol Using Corn Oil for Highly Flame-Retardant Polyurethane Foams, *C-Journal Carbon Res.* 5 (2019) 13.
- [28] U. Panchal, M.L. Chaudhary, P. Patel, J. Patel, R.K. Gupta, Soybean-Based Bio-Adhesives: Role of Diamine on the Adhesive Properties, *ACS Omega.* 9 (2024) 10738–10747.

- [29] P. Patel, R. Patel, J. Chaudhari, R.K. Gupta, Role of crosslinkers on the properties of bio-based wood adhesives, *Polym. Eng. Sci.* (2024) Just Accepted (10.1002/pen.26729).
- [30] F.E. Golling, R. Pires, A. Hecking, J. Weikard, F. Richter, K. Danielmeier, D. Dijkstra, Polyurethanes for coatings and adhesives – chemistry and applications, *Polym. Int.* 68 (2019) 848–855.
- [31] A. Das, P. Mahanwar, A brief discussion on advances in polyurethane applications, *Adv. Ind. Eng. Polym. Res.* 3 (2020) 93–101.
- [32] Y. Deng, R. Dewil, L. Appels, R. Ansart, J. Baeyens, Q. Kang, Reviewing the thermo-chemical recycling of waste polyurethane foam, *J. Environ. Manage.* 278 (2021) 111527.
- [33] C. Jayakody, D. Myers, C. Ogburn, Fire-Resistant Flexible Foams for High-Risk Cushioning Applications, (2005) 291–304.
- [34] W. Zatorski, Z.K. Brzozowski, A. Kolbrecki, New developments in chemical modification of fire-safe rigid polyurethane foams, *Polym. Degrad. Stab.* 93 (2008) 2071–2076.
- [35] A. Gomez-Lopez, B. Grignard, I. Calvo, C. Detrembleur, H. Sardon, Monocomponent Non-isocyanate Polyurethane Adhesives Based on a Sol-Gel Process, *ACS Appl. Polym. Mater.* 2 (2020) 1839–1847.
- [36] S. Wu, D. Deng, L. Zhou, P. Zhang, G. Tang, Flame retardancy and thermal degradation of rigid polyurethane foams composites based on aluminum hypophosphite, *Mater. Res. Express.* 6 (2019).
- [37] A. Yadav, F.M. de Souza, T. Dawsey, R.K. Gupta, Recent Advancements in Flame-Retardant Polyurethane Foams: A Review, *Ind. Eng. Chem. Res.* 61 (2022) 15046–15065.
- [38] A. Noreen, K.M. Zia, M. Zuber, S. Tabasum, A.F. Zahoor, Bio-based polyurethane: An efficient and environment friendly coating systems: A review, *Prog. Org. Coatings.* 91 (2016) 25–32.
- [39] V.K. Vijayan, Methyl isocyanate (MIC) exposure and its consequences on human health at Bhopal, *Int. J. Environ. Stud.* 67 (2010) 637–653.
- [40] P. Chemistry, R. Polyols, I. Acs, S. Series, A.C. Society, Foreword, *ACS Symp. Ser.* 1380 (2021).
- [41] S. Czlonka, A. Strakowska, A. Kairyte, Application of walnut shells-derived biopolyol in the synthesis of rigid polyurethane foams, *Materials (Basel)*. 13 (2020) 1–21.
- [42] A. Agrawal, R. Kaur, R.S. Walia, Investigation on flammability of rigid polyurethane foam-mineral fillers composite, *Fire Mater.* 43 (2019) 917–927.
- [43] R. Mohammadpour, G. Mir Mohamad Sadeghi, Effect of Liquefied Lignin Content

- on Synthesis of Bio-based Polyurethane Foam for Oil Adsorption Application, *J. Polym. Environ.* 28 (2020) 892–905.
- [44] L. Hojabri, X. Kong, S.S. Narine, Fatty Acid-Derived diisocyanate and biobased polyurethane produced from vegetable oil: Synthesis, polymerization, and characterization, *Biomacromolecules*. 10 (2009) 884–891.
- [45] D.P. Pfister, Y. Xia, R.C. Larock, Recent advances in vegetable oil-based polyurethanes, *ChemSusChem*. 4 (2011) 703–717.
- [46] C.E. Hoyle, C.N. Bowman, Thiol-ene click chemistry, *Angew. Chemie - Int. Ed.* 49 (2010) 1540–1573.
- [47] Z.S. Petrović, W. Zhang, I. Javni, Structure and properties of polyurethanes prepared from triglyceride polyols by ozonolysis, *Biomacromolecules*. 6 (2005) 713–719.
- [48] R.K. Gupta, M. Ionescu, X. Wan, D. Radojicic, N. Bilic, New polyols with isocyanuric structure by thiol-ene “click” chemistry reactions, *J. Cell. Plast.* 53 (2017) 639–662.
- [49] S. V. Levchik, E.D. Weil, Thermal decomposition, combustion and fire-retardancy of polyurethanes - A review of the recent literature, *Polym. Int.* 53 (2004) 1585–1610.
- [50] X. Peng, Z. Li, D. Wang, Z. Li, C. Liu, R. Wang, L. Jiang, Q. Liu, P. Zheng, A facile crosslinking strategy endows the traditional additive flame retardant with enormous flame retardancy improvement, *Chem. Eng. J.* 424 (2021) 130404.
- [51] F. Laoutid, L. Bonnaud, M. Alexandre, J.M. Lopez-Cuesta, P. Dubois, New prospects in flame retardant polymer materials: From fundamentals to nanocomposites, *Mater. Sci. Eng. R Reports*. 63 (2009) 100–125.
- [52] D.M. Hodgson, E. Gras, Recent developments in the chemistry of lithiated epoxides, *Synthesis (Stuttg)*. 27 (2002) 1625–1642.
- [53] M. Desroches, M. Escouvois, R. Auvergne, S. Caillol, B. Boutevin, From Vegetable Oils to Polyurethanes: Synthetic Routes to Polyols and Main Industrial Products, *Polym. Rev.* 52 (2012) 38–79.
- [54] V. Lenzi, A. Crema, S. Pyrlin, L. Marques, Current State and Perspectives of Simulation and Modeling of Aliphatic Isocyanates and Polyisocyanates, *Polymers (Basel)*. 14 (2022).
- [55] P. Furtwengler, L. Avérous, Renewable polyols for advanced polyurethane foams from diverse biomass resources, *Polym. Chem.* 9 (2018) 4258–4287.
- [56] H. Lim, S.H. Kim, B.K. Kim, Effects of silicon surfactant in rigid polyurethane foams, *Express Polym. Lett.* 2 (2008) 194–200.
- [57] M. Thirumal, D. Khastgir, G.B. Nando, Y.P. Naik, N.K. Singha, Halogen-free flame retardant PUF: Effect of melamine compounds on mechanical, thermal and

- flame retardant properties, *Polym. Degrad. Stab.* 95 (2010) 1138–1145.
- [58] Y. Liu, J. He, R. Yang, Effects of Dimethyl Methylphosphonate, Aluminum Hydroxide, Ammonium Polyphosphate, and Expandable Graphite on the Flame Retardancy and Thermal Properties of Polyisocyanurate-Polyurethane Foams, *Ind. Eng. Chem. Res.* 54 (2015) 5876–5884.
- [59] X. Hu, D. Wang, S. Wang, Synergistic effects of expandable graphite and dimethyl methyl phosphonate on the mechanical properties, fire behavior, and thermal stability of a polyisocyanurate-polyurethane foam, *Int. J. Min. Sci. Technol.* 23 (2013) 13–20.
- [60] W.H. Rao, Z.Y. Hu, H.X. Xu, Y.J. Xu, M. Qi, W. Liao, S. Xu, Y.Z. Wang, Flame-Retardant Flexible Polyurethane Foams with Highly Efficient Melamine Salt, *Ind. Eng. Chem. Res.* 56 (2017) 7112–7119.
- [61] A.S.A. Hazmi, M.M. Aung, L.C. Abdullah, M.Z. Salleh, M.H. Mahmood, Producing Jatropha oil-based polyol via epoxidation and ring opening, *Ind. Crops Prod.* 50 (2013) 563–567.
- [62] M.T. Benaniba, N. Belhaneche-Bensemra, G. Gelbard, Epoxidation of sunflower oil with peroxyacetic acid in presence of ion exchange resin by various processes, *Energy Educ. Sci. Technol.* 21 (2008) 71–82.
- [63] K.F. Adekunle, A Review of Vegetable Oil-Based Polymers: Synthesis and Applications, *Open J. Polym. Chem.* 05 (2015) 34–40.
- [64] M.J. Lerma-García, G. Ramis-Ramos, J.M. Herrero-Martínez, E.F. Simó-Alfonso, Authentication of extra virgin olive oils by Fourier-transform infrared spectroscopy, *Food Chem.* 118 (2010) 78–83.
- [65] P. Saha, B.S. Kim, Preparation, Characterization, and Antioxidant Activity of β -Carotene Impregnated Polyurethane Based on Epoxidized Soybean Oil and Malic Acid, *J. Polym. Environ.* 27 (2019) 2001–2016.
- [66] R. Gu, S. Konar, M. Sain, Preparation and characterization of sustainable polyurethane foams from soybean oils, *JAOCS, J. Am. Oil Chem. Soc.* 89 (2012) 2103–2111.
- [67] V.B. Borugadda, V. V. Goud, In-situ epoxidation of castor oil using heterogeneous acidic ion-exchange resin catalyst (IR-120) for bio-lubricant application, *Tribol. Online.* 10 (2015) 354–359.
- [68] K.P. Ang, C.S. Lee, S.F. Cheng, C.H. Chuah, Synthesis of palm oil-based polyester polyol for polyurethane adhesive production, *J. Appl. Polym. Sci.* 131 (2014) 1–8.
- [69] Z. Zhu, P. Lin, H. Wang, L. Wang, B. Yu, F. Yang, A facile one-step synthesis of highly efficient melamine salt reactive flame retardant for epoxy resin, *J. Mater. Sci.* 55 (2020) 12836–12847.
- [70] Y. Shi, Z. Wang, J.A. Zhou, Facile synthesis of a flame retardant melamine

- phenylphosphate and its epoxy resin composites with simultaneously improved flame retardancy, smoke suppression and water resistance, *RSC Adv.* 8 (2018) 39214–39221.
- [71] Y. Chen, Q. Wang, Preparation, properties and characterizations of halogen-free nitrogen–phosphorous flame-retarded glass fiber reinforced polyamide 6 composite, *Polym. Degrad. Stab.* 91 (2006) 2003.
- [72] D.W. Lachenmeier, H. Eberhard, F. Fang, S. Birk, D. Peter, S. Constanze, S. Manfred, NMR-spectroscopy for nontargeted screening and simultaneous quantification of health-relevant compounds in foods: The example of melamine, *J. Agric. Food Chem.* 57 (2009) 7194–7199.
- [73] N.M. Barkoula, B. Alcock, N.O. Cabrera, T. Peijs, Flame-Retardancy Properties of Intumescent Ammonium Poly(Phosphate) and Mineral Filler Magnesium Hydroxide in Combination with Graphene, *Polym. Polym. Compos.* 16 (2008) 101–113.
- [74] N. Elbers, C.K. Ranaweera, M. Ionescu, X. Wan, P.K. Kahol, R.K. Gupta, Synthesis of Novel Biobased Polyol via Thiol-Ene Chemistry for Rigid Polyurethane Foams, *J. Renew. Mater.* 5 (2017) 74–83.
- [75] M.A. Asare, P. Kote, S. Chaudhary, F.M. de Souza, R.K. Gupta, Sunflower Oil as a Renewable Resource for Polyurethane Foams: Effects of Flame-Retardants, *Polymers (Basel)*. 14 (2022) 5282.
- [76] Z. Zakaria, Z.M. Ariff, C.S. Sipaut, Effects of parameter changes on the structure and properties of low-density polyethylene foam, *J. Vinyl Addit. Technol.* 15 (2009) 120–128.
- [77] N.N. Najib, Z.M. Ariff, N.A. Manan, A.A. Bakar, C.S. Sipaut, Effect of Blowing Agent Concentration on Cell Morphology and Impact Properties of Natural Rubber Foam, *J. Phys. Sci.* 20 (2009) 13–25.
- [78] D.K. Chattopadhyay, D.C. Webster, Thermal stability and flame retardancy of polyurethanes, *Prog. Polym. Sci.* 34 (2009) 1068–1133.
- [79] D.K. Chattopadhyay, K.V.S.N. Raju, Structural engineering of polyurethane coatings for high performance applications, *Prog. Polym. Sci.* 32 (2007) 352–418.
- [80] L.G. Lage, Y. Kawano, Thermal degradation of biomedical polyurethanes—A kinetic study using high-resolution thermogravimetry, *J. Appl. Polym. Sci.* 79 (2001) 910–919.
- [81] X. Liu, J.J.-W. Hao, S. Gaan, Recent studies on the decomposition and strategies of smoke and toxicity suppression for polyurethane based materials, Royal Society of Chemistry, 2016.
- [82] A. König, U. Fehrenbacher, E. Kroke, T. Hirth, Thermal Decomposition Behavior of the Flame Retardant Melamine in Slabstock Flexible Polyurethane Foams, *J. Fire Sci.* 27 (2009) 187–211.

- [83] H.K. Lee, S.W. Ko, Structure and thermal properties of polyether polyurethaneurea elastomers, *J. Appl. Polym. Sci.* 50 (1993) 1269–1280.
- [84] J. Green, Mechanisms for flame retardancy and smoke suppression - A review, *J. Fire Sci.* 14 (1996) 426–442.